

# Long-term Averages of the Stochastic Logistic Map

Maricela Cruz and Austin Wei and Johanna Hardin and Ami Radunskaya

June 9, 2022

arXiv:2206.03849v1 [math.DS] 8 Jun 2022

# 1 Abstract

The logistic map is a nonlinear difference equation well studied in the literature, used to model self-limiting growth in certain populations. It is known that, under certain regularity conditions, the stochastic logistic map, where the parameter is varied according to a specified distribution, has a unique invariant distribution. In these cases we can compare the long-term behavior of the stochastic system with that of the deterministic system evaluated at the average parameter value. Here we examine the relationship between the mean of the stochastic logistic equation and the mean of orbits of the deterministic logistic equation at the expected value of the parameter. We show that, in some cases, the addition of noise is beneficial to the populations, in the sense that it increases the mean, while for other ranges of parameters it is detrimental. A conjecture based on numerical evidence presented at the end.

## 2 Introduction

The logistic map is a nonlinear first-order difference equation used to describe the evolution of many biological populations. It was first formulated by Pierre Francois Verhulst in 1838 [3] but became a phenomenon in the 1920's when it was rediscovered. Upon its rediscovery, it was often used to model many types of populations. As study of the logistic map continued, it was found that the map is a restricted special case of density-dependent population growth and hence, the model is not appropriate for many biological populations. However, the logistic map is still crucial in understanding more general models, and describes much of the qualitative behavior observed in population data. In particular, it captures both the stable and chaotic aspects of population growth. The logistic map has been extensively studied since the seminal work of Robert May [11]. For example, many protozoan populations such as yeast and grain beetles illustrate logistic growth in laboratory studies [12]. That is, for a specific set of parameters, protozoan populations may be stable, the populations stays the same size, but for a different set of parameters the population may exhibit chaotic behavior. Because the logistic map captures stable and chaotic behavior, it is used to explore how environmental change affects the growth of a population. When the growth rate has a stochastic component, reflecting realistic uncertainties in the environment, we would still like to understand the long term behavior of the system. Is there a stable distribution for the population? How does the long term behavior depend on the range of parameter values? Recently, Erguler and Stumpf used the stochastic logistic map to contrast the “true” dynamics of a system and observational noise, thereby addressing the reliability of inference from present data [7]. Diaconis and Freeman [6] develop a “contraction in the log average” criterion for the existence of a stable distribution of Markov processes. Arethreya and Dai have studied the random logistic map in particular [1] and have found situations in which there are multiple invariant measures, so that the long term behavior of the system depends on the initial state [2]. For a compendium of recent results and some new formulations, the reader is referred to [4, 10].

In this paper we present a new result that describes changes in the long term average of the logistic map when the parameter fluctuates in a specific range.

## 3 Background

### 3.1 The Map

The logistic map is a one-parameter family which gives the difference equation:

$$x_{n+1} = \lambda x_n(1 - x_n),$$

where  $x_n \in [0, 1]$  can be interpreted as a measure of the population in the  $n$ th time interval, and  $\lambda \geq 0$  represents the intrinsic growth rate.

In this paper, we discuss the logistic map under two different conditions, when  $\lambda$  is fixed and when it is random. In order to write out the map under the two conditions some notation is needed. Define,

$$\vec{\lambda} = (\lambda_1, \lambda_2, \dots); \lambda_i \stackrel{iid}{\sim} U(a, b) \text{ and}$$

$\sigma(\vec{\lambda})$  to be the shift operator such that  $\sigma : (\lambda_1, \lambda_2, \dots) \mapsto (\lambda_2, \lambda_3, \dots)$ . Let  $\pi(\vec{\lambda}) = \lambda_1$  be the projection onto the first coordinate of  $\vec{\lambda}$ . Then

$$S_\lambda(x) = \lambda x(1 - x) \tag{3.1}$$

denotes the logistic map when  $\lambda$  is fixed, and

$$T(\vec{\lambda}, x) = (\sigma(\vec{\lambda}), \pi(\vec{\lambda})x(1 - x)) \tag{3.2}$$

denotes the stochastic version of the logistic map as a skew product. Note that  $S_{\lambda_0}(x) = T(\vec{\lambda}, x)$  with  $\vec{\lambda} = (\lambda_0, \lambda_0, \lambda_0, \dots)$ . An example of the output of the stochastic logistic map is shown in Figure 1, where  $\lambda_i \stackrel{iid}{\sim} U(2, 2.5)$ .

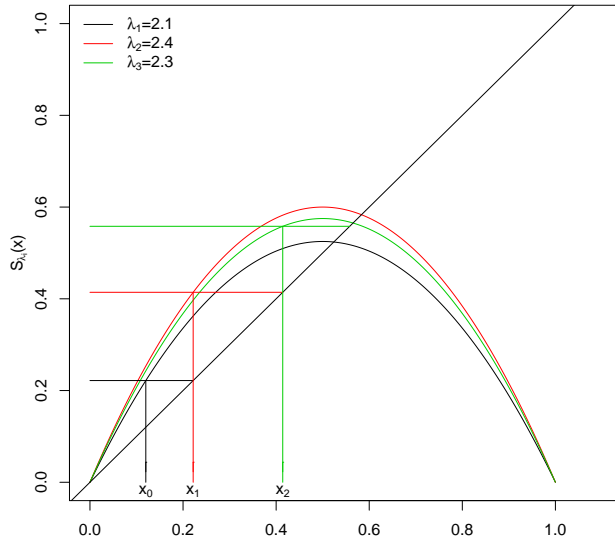


Figure 1:  $T^i(\vec{\lambda}, x_0)$  for  $i = 1, 2, 3$  where  $\vec{\lambda} = (2.1, 2.4, 2.3, \dots)$ , and  $x_0 = 0.12$ . The graphs of  $S_{2.1}(x)$ ,  $S_{2.4}(x)$  and  $S_{2.3}(x)$  are shown, with the line  $y = x$  superimposed.

We denote iterates of  $T(\vec{\lambda}, x)$  by  $T^i(\vec{\lambda}, x)$ , where

$$T^i(\vec{\lambda}, x) = T(T^{i-1}(\vec{\lambda}, x)) = (\sigma^i(\vec{\lambda}), \pi(\sigma^{i-1}(\vec{\lambda}))x(1-x)).$$

Define  $\Pi(\vec{\lambda}, x) = x$  as the projection of the pair  $(\vec{\lambda}, x)$  onto the state space,  $[0, 1]$ . We call the sequence  $x_0, x_1 = \Pi(T(\vec{\lambda}, x_0)), \dots, x_n = \Pi(T^n(\vec{\lambda}, x_0)), \dots$  the *orbit of  $x_0$*  under  $T(\vec{\lambda}, x)$ . If the initial value is a random variable independent of  $\lambda$ , then the set of orbits form a Markov Chain with state space some subset of  $[0, 1]$ , depending on the distribution of  $\lambda$ . We will use capital letters to denote this Markov Chain:  $X_1 = \Pi(T(\vec{\lambda}, X_0)), \dots, X_{i+1} = \Pi(T(\sigma^i(\vec{\lambda}), X_i))$ .

Note that in order to keep  $x$  in the interval  $[0, 1]$  for all iterations (to keep the unit interval invariant)  $\lambda$  must lie in the interval  $[0, 4]$ .

### 3.2 The Deterministic Logistic Map

Here we recall a few properties of the deterministic logistic map,  $S_\lambda(x)$ . For a more complete discussion see, for example, [11, 5, 14].

- For  $\lambda$  in the interval  $[0, 1]$ , 0 is the unique attracting fixed point of  $S_\lambda(x)$ , and, for every  $x_0 \in [0, 1]$ , the orbit  $\{x_n\} \rightarrow 0$  as  $n \rightarrow \infty$ .
- For  $\lambda$  in the interval  $(1, 3]$  there are two fixed points of  $S_\lambda(x)$  in  $[0, 1]$ :  $x^0 = 0$  and  $x^1 = \frac{\lambda-1}{\lambda}$ . In this regime, zero is an unstable fixed point, and  $x^1$  is attracting. For every  $x_0 \in (0, 1)$ , the orbit  $\{x_n\} \rightarrow x^1$ , the non-zero steady state. In other words, any initial distribution of  $x$ -values converges to a measure supported on a single point.
- For  $\lambda$  in the interval  $(3, 1 + \sqrt{6}]$ , the two fixed points (at zero and  $\frac{\lambda-1}{\lambda}$ ) are unstable, and the logistic map has a stable period-2 cycle. Almost all initial values in  $(0, 1)$  have orbits that converge to the period two orbit [14, p. 359]:

$$p(\lambda) = \frac{(\lambda+1) - \sqrt{(\lambda-3)(\lambda+1)}}{2\lambda} \quad (3.3)$$

$$q(\lambda) = \frac{(\lambda+1) + \sqrt{(\lambda-3)(\lambda+1)}}{2\lambda}. \quad (3.4)$$

Note the average along the period two orbit is  $\frac{\lambda+1}{2\lambda}$ , so that the long term average along almost every orbit is also  $\frac{\lambda+1}{2\lambda}$ .

- For  $\lambda$  in the interval  $(1 + \sqrt{6}, 3.54409]$  (approximately) both the fixed points and the period two cycle are unstable. However, the logistic map has a stable attracting period-4 cycle for parameter values in this interval: the population oscillates between 4 values. Almost all initial values of  $x_0 \in (0, 1)$  have orbits that converge to this period-4 cycle. Therefore, any initial continuous distribution of  $x$ -values will converge to a distribution supported on these four points.
- The parameter values at which the system transitions into the stable period 2-regime and into the stable period-4 regime are called *bifurcation points*. Define the parameter value  $\lambda_{c_k}$  to be the value at which bifurcation into a stable period  $k$  regime occurs. The first few bifurcation points can be

calculated as  $\lambda_{c_2} = 3$  and  $\lambda_{c_4} = 1 + \sqrt{6}$ . Since the period of the attracting cycle doubles at these points, the system is said to undergo a *period-doubling* bifurcation.

- Period doublings occur as  $\lambda$  increases. The bifurcation parameter values get closer and closer together, yielding stable cycles of period 8, 16, 32 and so on. As the period increases, the  $\lambda$ -interval between period doubling narrows. At  $\lambda_{c_{2^\omega}} = \lim_{n \rightarrow \infty} \lambda_{c_{2^n}} \approx 3.56995$ , stable periodic orbits of odd period appear in quick succession, according to Sarkovskii's theorem [5], culminating in a stable period-3 orbit at  $\lambda_{c_3} \approx 3.8284$ . After the period-3 region, the deterministic logistic map exhibits chaotic behavior [14].

The long term behavior of the logistic map  $S_\lambda(x)$  as  $\lambda$  varies between 0 and 4 can be depicted in a *bifurcation diagram*, as shown in Figure 2.

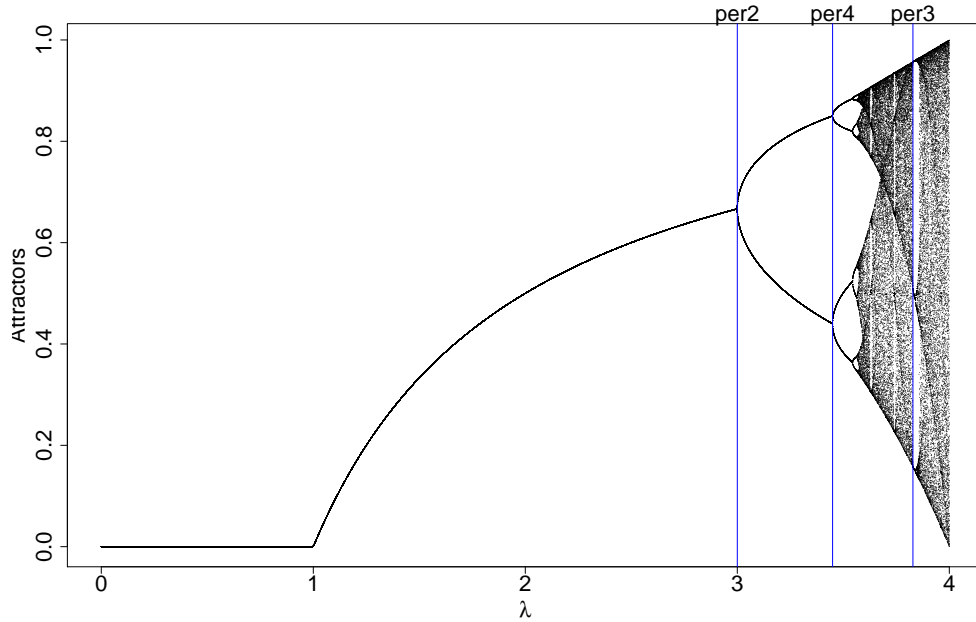


Figure 2: Bifurcation diagram for  $S_\lambda(x)$ . For each value of the parameter,  $\lambda$  One hundred initial values of  $x_0$  were generated uniformly on  $[0,1]$ . For each  $x_0$  value, the logistic map was iterated 1000 times for each  $\lambda$  on  $[0,4]$ , in increments of 0.001. The last iteration for each  $x_0$  at each  $\lambda$  is plotted. The bifurcation values for the period 2, period 4 and period 3 bifurcations are indicated as vertical lines.

### 3.3 Bifurcation Diagram for the Stochastic Logistic Map

We can numerically construct a bifurcation diagram for the stochastic logistic map by plotting the long-term behavior of a sample path as a function of the mean of a distribution of  $\lambda$ -values. Figure 3 shows an example of such a diagram where the parameter is uniformly distributed in a small interval:  $\lambda \sim \mathcal{U}([\bar{\lambda} - \Delta\lambda, \bar{\lambda} + \Delta\lambda])$ ,  $\Delta\lambda = 0.1$ , and  $\bar{\lambda}$  ranges from  $0 + \Delta\lambda = 0.1$  to  $4 - \Delta\lambda = 3.9$ . For  $\bar{\lambda} < 1 - \Delta\lambda = 0.9$ ,  $S_\lambda(x)$  has a unique attracting fixed point at  $x = 0$  for all  $\lambda \in (\bar{\lambda} - \Delta\lambda, \bar{\lambda} + \Delta\lambda)$ . Therefore, all orbits under  $T(\vec{\lambda}, x)$

converge to 0, and the bifurcation diagram in Figure 3 shows this with a horizontal line at 0 for  $\bar{\lambda} \in [0 + \Delta\lambda, 1 - \Delta\lambda]$ . For  $\bar{\lambda} \in (1 + \Delta\lambda = 1.1, 3 - \Delta\lambda = 2.9)$ ,  $S_\lambda(x)$  has a non-zero attracting fixed point at  $\frac{\lambda - 1}{\lambda}$  for all  $\lambda \in (\bar{\lambda} - \Delta\lambda, \bar{\lambda} + \Delta\lambda)$ . For these values of  $\bar{\lambda}$ , orbits of  $T(\bar{\lambda}, x)$  eventually enter the interval  $\left(\frac{\bar{\lambda} - \Delta\lambda - 1}{\bar{\lambda} - \Delta\lambda}, \frac{\bar{\lambda} + \Delta\lambda - 1}{\bar{\lambda} + \Delta\lambda}\right)$  with probability 1 and, once in this interval, they never leave it. Figure 3 shows a single curved strip of width  $\frac{2 \cdot \Delta\lambda}{(\lambda + \Delta\lambda)(\lambda - \Delta\lambda)}$  centered at  $\frac{\bar{\lambda}^2 - \bar{\lambda} - (\Delta\lambda)^2}{\bar{\lambda}^2 - (\Delta\lambda)^2}$ . Figure 3 also shows a distinct period 2 regime when  $\bar{\lambda} \in (3 + \Delta\lambda, 1 + \sqrt{6} - \Delta\lambda)$ .

Bifurcations of families of stochastic logistic maps have also been explored for other types of distributions of the parameter values. In [13], for example, the “dichotomous” case, where the distribution is supported on two  $\lambda$ -values, is studied. Implicit in the exploration of a stochastic system via these bifurcation diagrams (and, indeed, in the presentation of most numerical simulations of random phenomena) is that they represent generic behavior, i.e., that almost all orbits have the same limiting distribution: we would get roughly the same bifurcation diagram regardless of which value we chose for  $x_0$ . This characterizes *ergodicity*, which we define in the next section.

In the rest of this paper we are interested in statistical characterizations of orbits when  $\lambda$ -values are supported on small intervals that are completely contained in the stable periodic regimes of the deterministic logistic map. In particular, we consider the average behavior along orbits of the map  $T(\bar{\lambda}, x)$ , where  $\bar{\lambda}$  is an i.i.d. sequence of random variables  $\lambda_1, \lambda_2, \dots$  with common distribution  $g(\lambda)$ . In order to make statements about “the” average behavior, we need to establish the existence of a well-defined measure for the distribution of  $x$ -values after many iterations. This is the content of the next section.

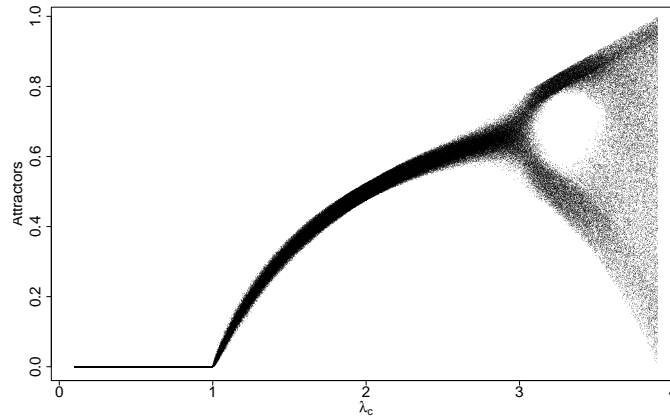


Figure 3: A bifurcation diagram for  $T(\bar{\lambda}, x)$  with  $\Delta\lambda = 0.1$  and  $\lambda_i \stackrel{i.i.d.}{\sim} \mathcal{U}(\bar{\lambda} - \Delta\lambda, \bar{\lambda} + \Delta\lambda)$ ,  $\bar{\lambda} \in [0 + \Delta\lambda, 4 - \Delta\lambda]$ . For each value of  $\bar{\lambda}$ , plotted on the horizontal axis, we begin with 100 values of  $x_0$  chosen from a uniform distribution on  $[0, 1]$ , and plot their  $1000^{th}$  iterate under  $T(\bar{\lambda}, x)$  on the vertical axis, where  $\bar{\lambda}$  is an i.i.d. sequence that is different for each simulation. In other words, we simulated 100 sample paths of the Markov Chain defined by the stochastic logistic map for each starting value,  $x_0$ . The periodic structure from the deterministic setting is still visible for  $\bar{\lambda}$ -values in the period-2 regime, but the bifurcations are blurred.

### 3.4 Ergodicity and Stability

We now consider the stochastic logistic map as a map on distributions. This requires some new definitions.

Let  $\mathcal{B}$  denote the Borel sigma-algebra on the state space  $\Omega = [0, 1]$  and  $\mathcal{M}$  the space of probability measures defined on  $(\Omega, \mathcal{B})$ . The stochastic map,  $T(\vec{\lambda}, x)$  induces a map on  $\mathcal{M}$  as follows. Assume that  $\vec{\lambda}$  is a sequence of i.i.d. random variables with common density  $g(\lambda)$  supported on  $[a, b] \subset [0, 4]$ . For  $\mu \in \mathcal{M}$  define the *Perron-Frobenius operator*

$$P^* \mu(A) = \int_0^4 \mu(S_\lambda^{-1}(A)) g(\lambda) d\lambda \quad (3.5)$$

Fixed points of this map take the place of fixed points in the deterministic setting.

**Definition 3.1** *An invariant measure is a measure  $\mu^* \in \mathcal{M}$ , such that,  $P^* \mu^*(A) = \mu^*(A)$  for all  $A \in \mathcal{B}$ .*

Thus, an invariant measure is a fixed point of the operator,  $P^*$ . We can also define stability for stochastic dynamical systems via the operator  $P^*$ :

**Definition 3.2** *Suppose  $\mu^*$  is the unique invariant measure for the operator  $P^*$ . Then the system  $T(\vec{\lambda}, x)$  is **stable in distribution** if, for any  $\mu \in \mathcal{M}$*

$$\left| \lim_{n \rightarrow \infty} (P^*)^n \mu(A) - \mu^*(A) \right| = 0, \quad \forall A \in \mathcal{B}$$

where  $P^*$  is the Perron-Frobenius operator associated with  $T$ .

A set  $A \in \mathcal{B}$  is invariant under  $T$  if  $T^{-1}(\vec{\lambda}, A) = A$ . A probability measure  $\mu$  is *ergodic* if  $\mu(A) = 0$  or 1 for every invariant set  $A$ . Suppose  $\mu^*$  is invariant and ergodic. Then  $\mu^*$  is the unique invariant probability, and the ergodic theorem tells us, that for any  $A \in \mathcal{B}$ , for almost every  $x_0$ , with respect to  $\mu^*$ :

$$\lim_{n \rightarrow \infty} \frac{1}{n} \sum_{i=0}^{n-1} \chi_A(x_i) = \mu^*(A), \quad (3.6)$$

where  $\chi_A(x)$  is the indicator function of the set  $A$  and  $\{x_i\}_{i=0}^\infty$  is an orbit of  $x_0$  under the stochastic map. If, in addition, the invariant measure  $\mu^*$  is stable, then

$$\mu^*(A) = \lim_{n \rightarrow \infty} (P^*)^n \mu(A), \quad \forall \mu \in \mathcal{M}.$$

Thus, we can estimate the long-term behavior along a  $\mu^*$ -generic orbit by iterating simulated estimates of arbitrary distributions. In fact, this is the justification behind the algorithm used to generate the stochastic bifurcation diagram shown in Figure 3.

The following result from [4, p. 343] shows that the stochastic logistic map with continuous parameter distributions supported in a given periodic regime is stable.

Assume that  $S_\lambda(x)$  has a stable periodic orbit with period  $m$  for all  $\lambda$  in the support of  $g(\lambda)$ .

**Proposition 3.3** [4] *If*

$$E[\log \lambda] > 0 \text{ and } E[|\log(4 - \lambda)|] < \infty$$

*then*

1. *the stochastic dynamical system  $T(\vec{\lambda}, x)$  has a unique invariant probability measure  $\mu^* \in \mathcal{M}$ , and*
2.  $\left| \lim_{n \rightarrow \infty} (P^*)^{mn} \mu(A) - \mu^*(A) \right| = 0$  *for all  $A \in \mathcal{B}, \mu \in \mathcal{M}$ .*

In this paper, we consider the situation when  $g(\lambda)$  is the uniform density on an interval  $[a, b]$ , where  $[a, b]$  is entirely within either the non-zero fixed point regime:  $(1, 3)$ , the period-2 regime:  $(3, 1 + \sqrt{6})$ , or the period-4 regime:  $(1 + \sqrt{6}, 3.54409)$ . In all cases,  $a$  and  $b$  are bounded away from 1 and 4, so that  $E[\log \lambda] > 0$  and  $E[|\log(4 - \lambda)|] < \infty$ . Therefore, Proposition 3.3 applies and we know that the long-term distribution of almost all orbits is well-defined. Thus, “the expected value” exists in the various periodic regimes, and we are in a position to compare the means of the deterministic and stochastic logistic maps in these regimes. Note that we do not have an explicit formula for the unique invariant measure, but its existence and stability ensure that numerical simulations should reflect the generic behavior of sample paths of the system.

We can verify the theoretical results numerically by exploring more closely “slices” of the stochastic bifurcation diagram shown in Figure 3.

The red-solid densities in Figure 4 represent three different slices (panel (a), (b), and (c), respectively) of the bifurcation diagram of  $T(\vec{\lambda}, x)$  shown in Figure 3 using  $\Delta\lambda = 0.024$ , with  $\lambda$ -values supported in different periodic regions. Plot (a) is a vertical slice of a bifurcation diagram of  $T(\vec{\lambda}, x)$  with  $\lambda \sim \mathcal{U}[1.508 - \Delta\lambda, 1.508 + \Delta\lambda]$ , within the non-zero fixed point regime. The figure shows the empirical distribution of the  $x$  values for different iterations, i.e., it gives a numerical approximation of iterates of the Perron-Frobenius operator,  $P^*$  given in Equation (3.5), applied to the uniform distribution. To generate the numerical approximation, we start with 1000 uniformly drawn random values of  $X_0$ . This gives a numerical approximation to  $\mu$ , the uniform distribution on  $[0, 1]$  indicated by the purple-two-dash curve in Figure 4. The blue-long-dash curve in panel (a) represents the empirical distribution of  $X_1 = T(\vec{\lambda}, X_0)$  with  $\lambda \sim \mathcal{U}[1.508 - \Delta\lambda, 1.508 + \Delta\lambda]$ . The other curves give the empirical distributions of  $X_{10}, X_{50}, X_{100}$  and finally  $X_{1000}$ , in red-solid. Plots (b) and (c) show the evolution of the uniform distribution under  $P^*$  when the parameter values are in the period-2 and period-4 regions; the distributions were created using  $\lambda \sim \mathcal{U}[3.208 - \Delta\lambda, 3.208 + \Delta\lambda]$  and  $\lambda \sim \mathcal{U}[3.508 - \Delta\lambda, 3.508 + \Delta\lambda]$ , respectively. The periodicity of the deterministic systems is reflected in the multi-modality of the limiting distributions, although we note that these empirically derived distributions suggest asymmetries. These numerical results also suggest that the 50th iteration of  $P^*$  gives a fairly close approximation to the stable invariant distribution,  $\mu^*$ . The choice of  $\Delta\lambda = 0.024$  was made so that the visual intuition becomes clear, but the theoretical results do not depend on any specific value of  $\Delta\lambda$ .

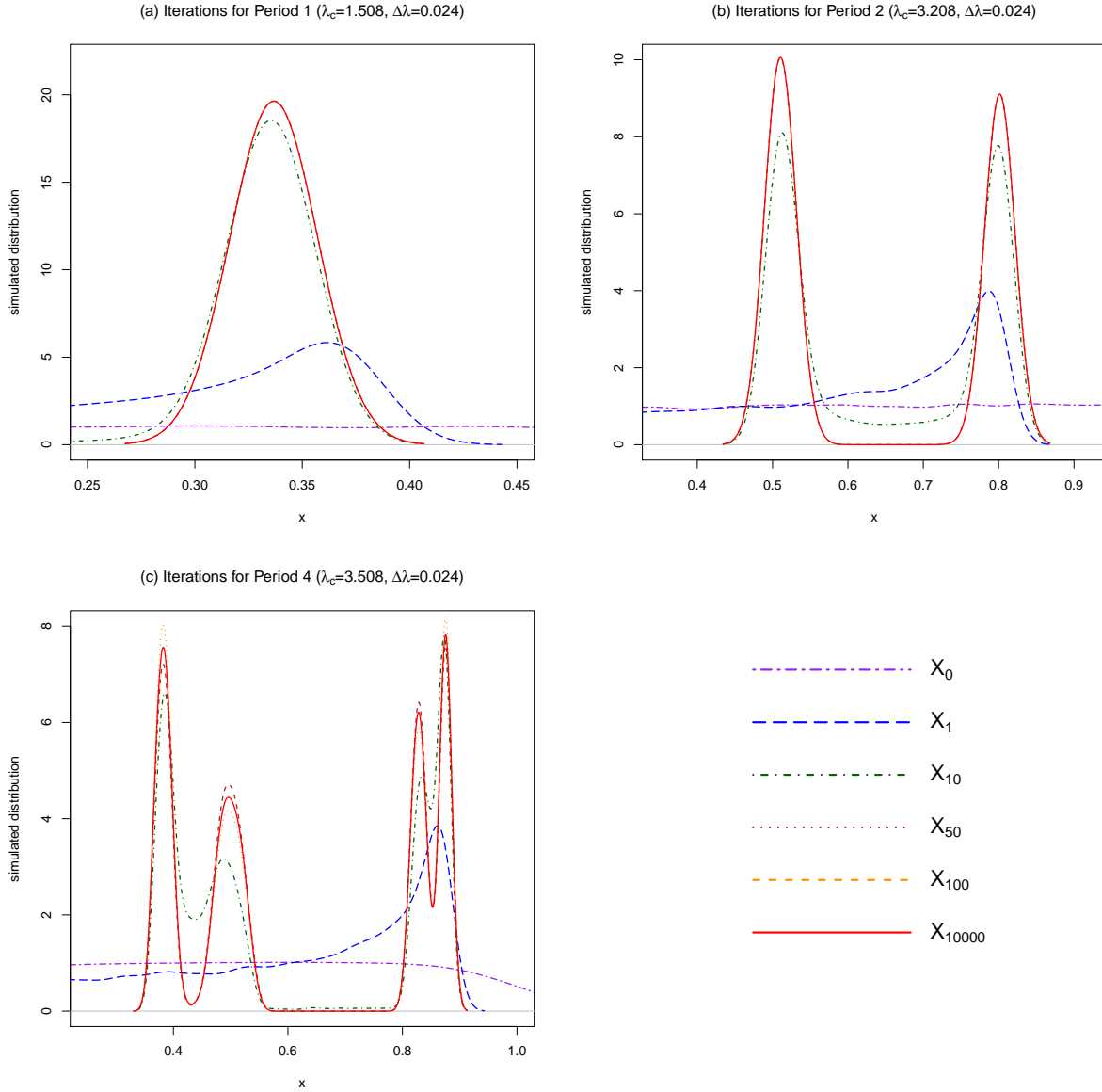


Figure 4: The distribution of the state variable with a uniform initial distribution. The initial, 1st, 10th, 50th, 100th, and 10000th iterations are shown in purple-two-dash, blue-long-dash, green-dog-dash, brown-dot-dot, orange-dash, and red-solid respectively. The parameter values in each of the three plots are distributed according to (a)  $\lambda \sim \mathcal{U}[1.508 - \Delta\lambda, 1.508 + \Delta\lambda]$ , (b)  $\lambda \sim \mathcal{U}[3.208 - \Delta\lambda, 3.208 + \Delta\lambda]$ , and (c)  $\lambda \sim \mathcal{U}[3.508 - \Delta\lambda, 3.508 + \Delta\lambda]$ . Note that the red-solid densities in each plot give an empirical estimate of the invariant distribution for the given distribution on  $\lambda$ .

## 4 Stochastically-induced changes in the average behavior.

### 4.1 Mean versus Mean

If  $g(\lambda)$  has support in one of the periodic regimes, then Proposition 3.3 gives (let  $A = (0, 1)$ ):

$$\lim_{n \rightarrow \infty} \frac{1}{n} \sum_{i=0}^{n-1} T^i(\vec{\lambda}, x) = \int_0^1 x d\mu^*(x) = E_{\mu^*}[X],$$

for almost all initial values of  $x$ .

The goal of this paper is to compare the expected value of  $X$  under  $T(\vec{\lambda}, \cdot)$  with the mean along the periodic orbit under  $S_{\lambda}(x) = \lambda x(1 - x)$ , the deterministic map, using the expected value of  $\lambda$ . Similar investigations have been discussed in [8] in the context of the Beverton-Holt equation, and in [9], in the context of self-limiting exponential growth. In the next section we compare the average behavior of the stochastic logistic map with the deterministic map in several parameter regimes, uncovering a pattern of alternating larger and smaller expected values under stochasticity.

### 4.2 Period One

Suppose  $\lambda \sim \mathcal{U}([a, b])$ . In Figure 5 we compare the “deterministic mean”, i.e., the long term average of orbits under  $S_{\bar{\lambda}}$  where  $\bar{\lambda} = \frac{a+b}{2}$ , with the long term behavior under the stochastic dynamical system,  $T(\vec{\lambda}, \cdot)$ . The left panel of Figure 5 shows the stable fixed point at  $\bar{\lambda} = 1.508$  (red line), the limit set for almost all orbits under  $S_{\bar{\lambda}}$ . In the same panel we plot the empirical distribution of  $(P^*)^{10000}(\mu)$  (black histogram), where  $\mu$  is the uniform distribution on  $(0, 1)$ ,  $\Delta\lambda = 0.024$ , and  $\lambda \sim \mathcal{U}([1.508 - \Delta\lambda, 1.508 + \Delta\lambda])$ ; the average of the empirical distribution is given by the blue line. Because the system is stable, we can interpret  $(P^*)^{10000}(\mu)$  as an estimate of the invariant distribution,  $\mu^*$ . The right panel of Figure 5 shows a magnification of the left panel. Observe that the blue line is to the left of the red line, hence the (empirically estimated) average of  $\mu^*$  is less than the stable fixed point of the deterministic map when  $\bar{\lambda} = 1.508$ . Since the stable fixed point is the average along almost every orbit of the deterministic map, Figure 5 gives a visual comparison of the mean of the stochastic system, where the parameter values have mean  $\bar{\lambda}$  (blue line), with the mean of the deterministic system with parameter value equal to  $\bar{\lambda}$  (red line).

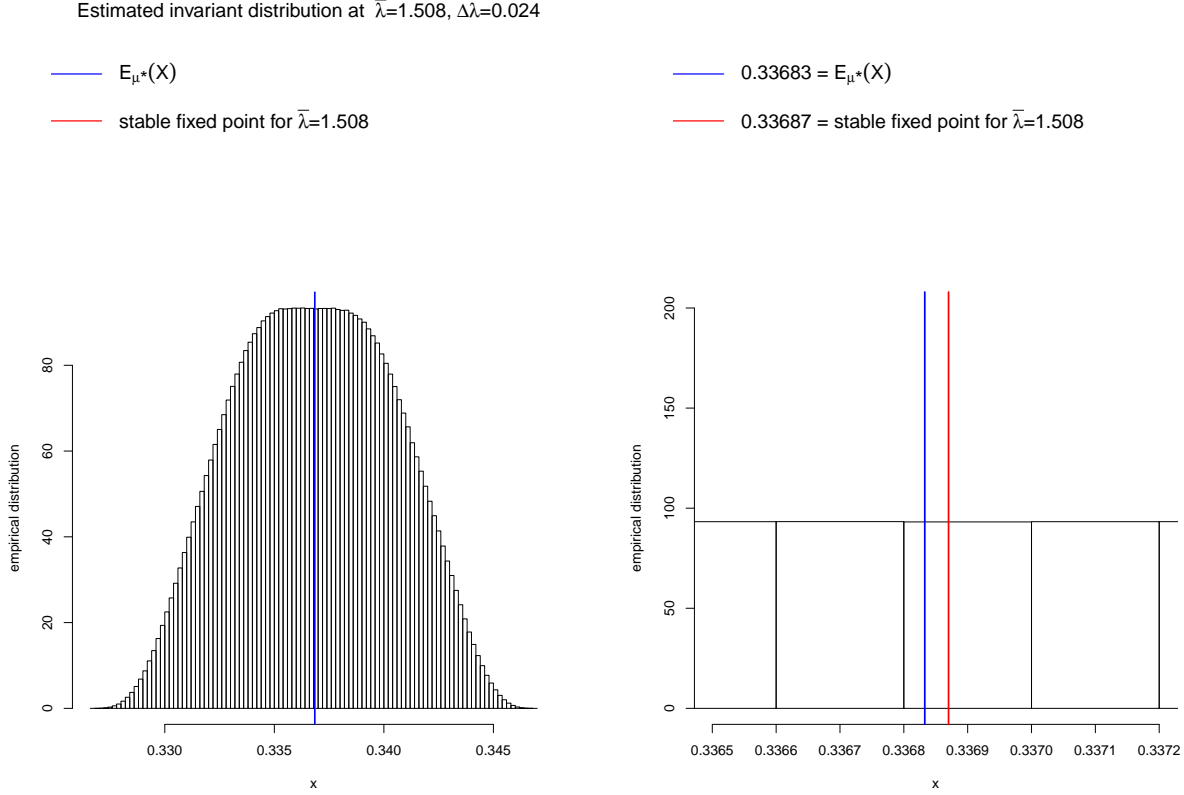


Figure 5: Numerically estimated histogram of the 10000<sup>th</sup> iterate of  $P^*$ , the Perron-Frobenius operator associated with  $T(\bar{\lambda}, x)$ . In this simulation, the parameter value at each iteration is given by  $\lambda \sim U[1.508 - \Delta\lambda, 1.508 + \Delta\lambda]$  with  $\Delta\lambda = 0.024$ ; 20,000 initial  $x$ -values were drawn from a uniform distribution on  $[0, 1]$ . Since the system has a unique stable invariant measure, the histogram is an estimate of the distribution of the limiting invariant measure,  $\mu^*$ . The right panel shows a magnification of the central portion of the histogram, highlighting that the mean of the empirical histogram (blue line) is less than the stable fixed point of the logistic map with the average parameter value,  $\bar{\lambda} = 1.508$  (red line).

The following theorem, a straightforward application of Jensen’s inequality, shows that the “stochastic mean” will always be less than the deterministic mean. In other words, the presence of randomness lowers the long term average in the period-one regime.

Define  $x^*(\lambda) = \frac{\lambda - 1}{\lambda}$  to be the non-zero fixed point of the map  $S_\lambda(x)$ . Recall that this fixed point is *attracting* for  $\lambda \in (1, 3)$  and, therefore, the Cesaro average along almost any orbit converges to  $x^*(\lambda)$ :

$$\lim_{n \rightarrow \infty} \frac{1}{n} \sum_{i=0}^{n-1} S_\lambda^i(x) = \frac{\lambda - 1}{\lambda} = x^*(\lambda) \quad \text{if } \lambda \in (1, 3).$$

**Theorem 4.1** Let  $g(\lambda)$  be a continuous density whose support is in the period one region,  $(1, 3)$ . Then the mean of  $X$  under the stochastic logistic map  $T(\vec{\lambda}, \cdot)$  is **less** than the stable fixed point of the deterministic map  $S_{\bar{\lambda}}(x)$ , where  $\bar{\lambda} = \int_0^4 \lambda g(\lambda) d\lambda$ .

**Proof** Let  $\mu^*$  be the unique invariant distribution of the Perron-Frobenius operator associated with  $T(\vec{\lambda}, \cdot)$ . Since  $\lambda$  is independent of  $X$ :

$$\begin{aligned}
E_{\mu^*}(X) &= \int_0^1 x d\mu^*(x) \\
&= \int_0^1 x dP^*(\mu^*)(x) \\
&= \int_0^1 \int_0^4 \lambda x(1-x) g(\lambda) d\lambda d\mu^*(x) \\
&= \bar{\lambda} \int_0^1 x - x^2 d\mu^*(x) \\
&= \bar{\lambda} (E_{\mu^*}(X) - E_{\mu^*}(X^2)) \\
&\leq \bar{\lambda} (E_{\mu^*}(X) - E_{\mu^*}(X)^2) \quad \text{since, by Jensen's inequality } E_{\mu^*}(X)^2 \leq E_{\mu^*}(X^2)
\end{aligned}$$

$$\begin{aligned}
&\Rightarrow (\bar{\lambda} - 1)E_{\mu^*}(X) - \bar{\lambda}E_{\mu^*}^2(X) \geq 0 \\
&\Rightarrow E_{\mu^*}(X) (\bar{\lambda} - 1 - \bar{\lambda}E_{\mu^*}(X)) \geq 0 \\
&\Rightarrow E_{\mu^*}(X) \leq \frac{\bar{\lambda}-1}{\bar{\lambda}} = x^*(\bar{\lambda})
\end{aligned}$$

since  $E_{\mu^*}(X) \geq 0$ . Furthermore, the inequality is strict unless  $E_{\mu^*}(X^2) = 0$ . ■

Note: the final inequality in the proof of Theorem 4.1 holds for  $\lambda$  in any region. However,  $\frac{\bar{\lambda} - 1}{\bar{\lambda}}$  is the average of the deterministic system only in the non-zero stable period-one regime,  $\lambda \in (1, 3)$ . Therefore, the proof of theorem 4.1 does not tell us anything about the relationship between the stochastic and deterministic means when  $g(\lambda)$  is supported in other regions.

### 4.3 Period Two

Figure 6 shows a histogram of  $(P^*)^{10000}(\mu) \approx \mu^*$  where the parameter values have a uniform distribution:  $\lambda \sim \mathcal{U}([3.208 - \Delta\lambda, 3.208 + \Delta\lambda])$ ,  $\Delta\lambda = 0.024$ . As in Figure 5, the empirical stochastic and deterministic means with  $\bar{\lambda} = 3.208$  are indicated by green and orange vertical lines, respectively. The right panel of Figure 6 shows a magnified region of the left panel, showing that the orange line is to the left of the green line, so the empirical estimate of the stochastic mean is *greater* than the average along the entire stable period-2 orbit of the average parameter value. Note that this is opposite of the situation depicted in Figure 5. The numerical results, along with other simulated histograms of  $(P^*)^{10000}(\mu)$  (not shown) when  $\lambda$  is in the period two region, suggest that the expected value of  $\pi(T(\vec{\lambda}, X))$  is **greater** than the mean along the stable period-2 orbit of the deterministic map evaluated at  $\bar{\lambda}$ . In other words, the relationship between the stochastic and deterministic means in the period two region is the reverse of the relationship in the period one region. We prove that this is the case in Theorem 4.2.

We can gain some intuition about this reversal from the following observation, also depicted in Figure 6. For  $\lambda \in [3.208 - \Delta\lambda, 3.208 + \Delta\lambda]$ , the map  $S_\lambda$  has a stable period 2 orbit:  $\{p(\lambda), q(\lambda)\}$  where  $p(\lambda) < q(\lambda)$  are given by Equations (3.3) and (3.4), respectively. Thus, almost all orbits of the stochastic system will eventually enter two disjoint intervals,  $I_p$  and  $I_q$ , where  $I_q$  is the image of the interval:  $[p(3.208 + \Delta\lambda), p(3.208 - \Delta\lambda)]$  and  $I_p$  is the image of the interval  $[q(3.208 - \Delta\lambda), q(3.208 + \Delta\lambda)]$ . A generic orbit will alternately visit  $I_p$  and  $I_q$  and thus the invariant measure,  $\mu^*$ , can be written as a sum of two measures,  $\mu_p^*$  and  $\mu_q^*$ , supported on  $I_p$  and  $I_q$ , respectively, and  $E_{\mu^*}(X)$  will be the average of  $E_{\mu_p^*}(X)$  and  $E_{\mu_q^*}(X)$ . Figure 6 compares  $E_{\mu_p^*}(X)$  and  $E_{\mu_q^*}(X)$  with the stable period-2 points of the deterministic system with the average parameter value,  $\bar{\lambda} = 3.208$ . We see that  $E_{\mu_p^*}(X) > p(\bar{\lambda})$  and  $E_{\mu_q^*}(X) < q(\bar{\lambda})$ , but we show in the Appendix that the first inequality is larger than the second, so that  $E_{\mu^*}(X) > \frac{p(\bar{\lambda}) + q(\bar{\lambda})}{2}$ . This is the conclusion of Theorem 4.2.

Estimated invariant distribution at  $\bar{\lambda}=3.208$ ,  $\Delta\lambda=0.024$

- $E_{\mu_p}(X)$  and  $E_{\mu_q}(X)$
- stable period 2 points  $(p(\bar{\lambda}) \text{ \& } q(\bar{\lambda}))$  with  $\bar{\lambda}=3.208$
- $E_{\mu^*}(X)=(E_{\mu_p}(X) + E_{\mu_q}(X))/2$
- $(p(\bar{\lambda}) + q(\bar{\lambda}))/2$  with  $\bar{\lambda}=3.208$
- $0.65593=E_{\mu^*}(X)=(E_{\mu_p}(X) + E_{\mu_q}(X))/2$
- $0.65586=(p(\bar{\lambda}) + q(\bar{\lambda}))/2$  with  $\bar{\lambda}=3.208$

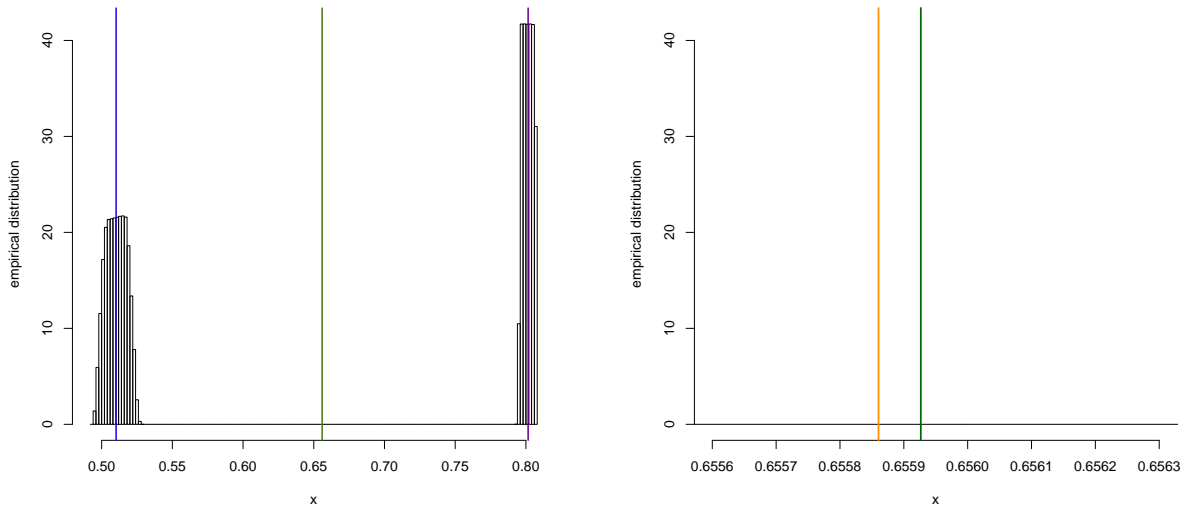


Figure 6: Numerically estimated histogram of the 10000<sup>th</sup> iterate of  $P^*$ , the Perron-Frobenius operator associated with  $T(\bar{\lambda}, x)$ . In this simulation, the parameter value at each iteration is given by  $\lambda \sim U[3.208 - \Delta\lambda, 3.208 + \Delta\lambda]$  with  $\Delta\lambda = 0.024$ ; 20,000 initial  $x$ -values were drawn from a uniform distribution on  $[0, 1]$ . Since the system has a unique stable invariant measure, this histogram is an estimate of the distribution of the limiting invariant measure,  $\mu^*$ . The right panel shows a magnification of the central portion of the bimodal histogram, highlighting that the mean of the empirical histogram (green line,  $(E_{\mu_p^*}(X) + E_{\mu_q^*}(X))/2$ ) is greater than the average of the stable fixed points of the invariant distribution at the average parameter value,  $\bar{\lambda} = 3.208$  (orange line,  $(p(\bar{\lambda}) + q(\bar{\lambda}))/2$ ).

The previous observation motivates the following theorem. While it seems that the theorem should be true based on a convexity argument similar to the one used to prove Theorem 4.1, the proof presented here relies on several rather technical lemmas which are proved in the Appendix. Perhaps in the future a simpler proof will be found. Further speculation in this direction is undertaken in the Discussion section at the end of the

paper.

**Theorem 4.2** *In the period two region,  $\lambda \in (3, 1 + \sqrt{6})$ , the expected value of  $X$  under  $\mu^*$ , the stochastic logistic map (i.e.,  $\Delta\lambda > 0$ ), is **greater** than the average of the stable period-2 points of the deterministic map with the average parameter value,  $\bar{\lambda}$ .*

$$E_{\mu^*}(X) > \frac{p(\bar{\lambda}) + q(\bar{\lambda})}{2} = \frac{\bar{\lambda} + 1}{2\bar{\lambda}}$$

Suppose  $\lambda \sim \mathcal{U}(\bar{\lambda} - \Delta\lambda, \bar{\lambda} + \Delta\lambda)$  where  $(\bar{\lambda} - \Delta\lambda, \bar{\lambda} + \Delta\lambda) \subset (3, 1 + \sqrt{6})$  and  $\Delta\lambda$  is small enough so that the support of the invariant distribution,  $\mu^*$ , consists of two disjoint intervals (see Lemma 6.1 in the Appendix). Then define the measures  $\mu_p^*$  and  $\mu_q^*$  as follows:

$$\mu_p^*(A) = 2\mu^*\left(A \cap \left[0, \frac{\bar{\lambda} - 1}{\bar{\lambda}}\right]\right) \quad \mu_q^*(A) = 2\mu^*\left(A \cap \left(\frac{\bar{\lambda} - 1}{\bar{\lambda}}, 1\right]\right) \quad (4.1)$$

Thus,  $\mu_p^*$  gives the left peak of the invariant distribution, and  $\mu_q^*$  gives the right peak.

The proof of Theorem 4.2 involves showing that, for small  $\Delta\lambda > 0$ , the expected value of the lower peak,  $E_{\mu_p^*}[X]$ , is farther from  $p(\bar{\lambda})$  than the distance of the expected value of the upper peak,  $E_{\mu_q^*}[X]$ , to  $q(\bar{\lambda})$ . The entire proof is in the Appendix.

#### 4.4 Period Four

Figure 7 shows the average of the four stable fixed points for  $\bar{\lambda} = 3.508$ , corresponding to the four points on the vertical slice of the bifurcation diagram (see Figure 2) of  $S_\lambda(x)$  with  $\lambda = 3.508$  (orange line). In the same figure, we plot the average of the points that make up the empirical histogram (green line). Observe in the right panel of Figure 7, the zoomed in version of the left panel, the  $x$ -coordinate of the green line is less than that of the orange line, so the average of the empirical estimation of  $\mu^*$  is strictly less than the average of the stable period-four points, just as in the period one region. Figure 7, and other histograms of the last four iterations (not shown) of  $T(\bar{\lambda}, x)$  for  $\lambda$  in the period four region, suggest that the expected value of  $\mu^*$  under the stochastic logistic map is **less** than or equal to the long term average under the corresponding deterministic map.

Estimated invariant distribution at  $\bar{\lambda}=3.508$ ,  $\Delta\lambda=0.024$

- $E_{\mu^*}(X)$  restricted
  - stable period 4 points for  $\bar{\lambda}=3.508$
  - $E_{\mu^*}(X)$
  - average of stable period 4 points for  $\bar{\lambda}=3.508$
- $0.6462 = E_{\mu^*}(X)$
  - $0.6466 =$  average of stable fixed points for  $\bar{\lambda}=3.508$

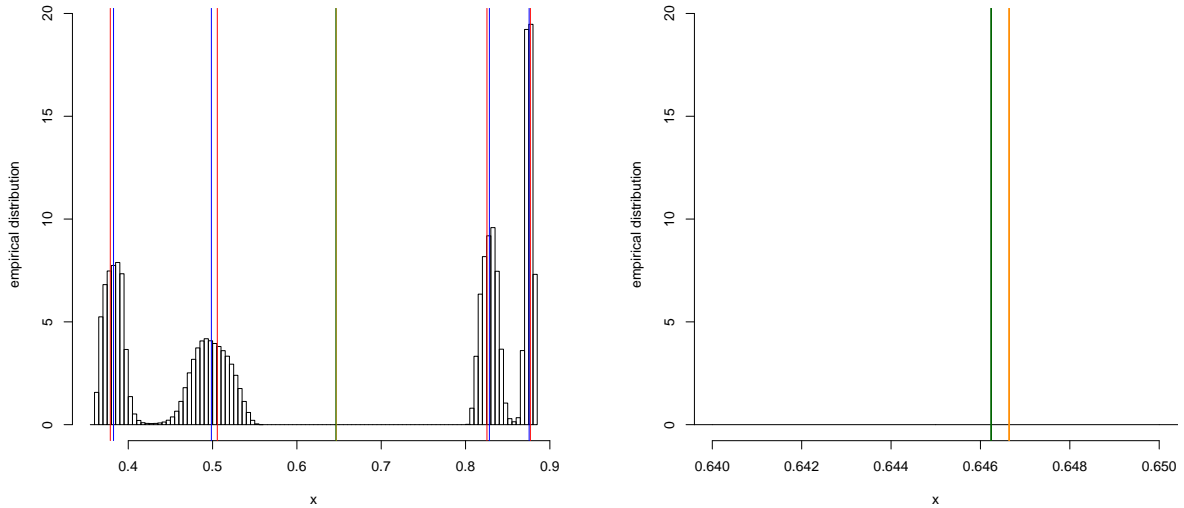


Figure 7: Numerically estimated histogram of the 10000<sup>th</sup> iterate of  $P^*$ , the Perron-Frobenius operator associated with  $T(\bar{\lambda}, x)$ . In this simulation, the parameter value at each iteration is given by  $\lambda \sim U[3.508 - \Delta\lambda, 3.508 + \Delta\lambda]$  with  $\Delta\lambda = 0.024$ ; 20,000 initial  $x$ -values were drawn from a uniform distribution on  $[0, 1]$ . Since the system has a unique stable invariant measure, this histogram is an estimate of the distribution of the limiting invariant measure,  $\mu^*$ . The right panel shows a magnification of the central portion of the histogram, highlighting that the mean of the empirical histogram (green line) is less than the average of the stable fixed points of the invariant distribution at the average parameter value,  $\bar{\lambda} = 3.508$  (orange line).

## 5 Discussion

Previous studies have explored the effect of randomness on the average behavior of families of one-dimensional maps with stable fixed points [8, 9]. In this paper we compared the expected value of the deterministic and stochastic logistic map in different periodic regimes. We showed that a unique stable invariant measure existed under the Perron-Frobenius map associated with the stochastic logistic map in the parameter

regions of interest. This allowed us to interpret numerical experiments, and allowed us to compare the expected value of the stochastic logistic map with that of the deterministic map.

In the period one region, the average of the deterministic map, which is the fixed point of the map at the average parameter values, is greater than the expected value of  $X$  under the unique stable invariant distribution of the stochastic map. Since this distribution is stable, the long term average of almost all orbits under  $T(\bar{\lambda}, x)$  is strictly less than the long-term average under the related deterministic map. In terms of a growth model, if an environmental parameter that affects the birth rate of the population fluctuates randomly around a mean value  $\bar{\lambda}$ , then the average population will be smaller than in the deterministic model with parameter fixed at  $\bar{\lambda}$ .

These results for the period one region are similar to those in [8], which apply to the stochastic Beverton-Holt model. This is not surprising, since the proof of Theorem 4.1 uses only the fact that the logistic map is unimodal and concave down, features shared by the Beverton-Holt model. In [9] a similar result is proved in greater generality, allowing for arbitrary distributions of the parameter.

In contrast to the period one region, in the period two region the average of the deterministic map is **less** than the expected value of  $X$  under the unique stable invariant distribution of the stochastic map. The period two result is given in Theorem 4.2 and proved in the Appendix. The switch in behavior led us to explore what happens after further period doubling bifurcations.

Our empirical simulations (shown in Figure 7) demonstrate that the behavior in the period four region reverts to that of the period one region. In particular, it seems as though the average of the deterministic map is again greater than the expected value of  $X$  under the unique stable invariant distribution of the stochastic map. The oscillating behavior across the different regions leads us to the following “flip-flop” conjecture.

**Conjecture 5.1** *Flip-flop conjecture.*

1. For  $\rho$  **odd**, consider regions with period  $2^\rho$ . Let  $p_i(\bar{\lambda})$  be the stable period- $2^\rho$  points of the deterministic map with the average parameter value,  $\bar{\lambda}$ .

*The expected value of  $X$  under the stochastic logistic map is **greater** than the average of the stable period- $2^\rho$  points of the deterministic map with the average parameter value,  $\bar{\lambda}$ .*

$$E_{\mu^*}(X) > \frac{1}{2^\rho} \sum_{i=1}^{2^\rho} p_i(\bar{\lambda})$$

2. For  $\rho$  **even**, consider regions with period  $2^\rho$ . Let  $p_i(\bar{\lambda})$  be the stable period- $2^\rho$  points of the deterministic map with the average parameter value,  $\bar{\lambda}$ .

*The expected value of  $X$  under the stochastic logistic map is **less** than the average of the stable period- $2^\rho$  points of the deterministic map with the average parameter value,  $\bar{\lambda}$ .*

$$E_{\mu^*}(X) < \frac{1}{2^\rho} \sum_{i=1}^{2^\rho} p_i(\bar{\lambda})$$

We note that a renormalization argument might be used to explore the conjecture, since the convexity of the iterates:  $S_\lambda(x)$ ,  $S_\lambda^2(x)$ ,  $S_\lambda^4(x)$ ,  $\dots$  at the fixed point switches as the number of iterates is doubled. Thus, it

makes sense to conjecture that as we increase the period, the direction of the inequality switches back and forth, at least through the period doubling range of  $\lambda$ . We hope to explore this direction in future work.

## 6 Appendix

This Appendix contains the proof of the main result of the paper, Theorem 4.2. The proof consists of a series of lemmas. To guide the reader and to highlight the steps in the argument, we first provide an outline of the lemmas.

Recall Theorem 4.2:

In the period two region,  $\lambda \in (3, 1 + \sqrt{6})$ , the expected value of  $X$  under  $\mu^*$  (the stochastic logistic map) is **greater** than the average of the stable period-2 points of the deterministic map with the average parameter value,  $\bar{\lambda}$ .

$$E_{\mu^*}(X) > \frac{p(\bar{\lambda}) + q(\bar{\lambda})}{2} = \frac{\bar{\lambda} + 1}{2\bar{\lambda}}$$

1. First, we establish that, for small amplitudes of noise, the support of the invariant measure is contained in two disjoint intervals (**Lemma 6.1**).
2. The expected value of  $X$  with respect to the right hand measure (as defined in Equation (4.1)) is the same as the expected value of the first iterate of the deterministic map at  $\bar{\lambda}$  with respect to the left hand measure (**Lemma 6.2**).

$$E_{\mu_q^*}[X] = E_{\mu_p^*}[S_{\bar{\lambda}}(X)]$$

3. The left peak of the invariant measure, i.e., the expected value with respect to  $\mu_p^*$ , is larger than the smaller point on the period-2 cycle of  $S_{\bar{\lambda}}$  (**Lemma 6.3**).

$$E_{\mu_p^*}[X] > p(\bar{\lambda})$$

To prove Lemma 6.3: create functions  $H$  and  $F$ , apply Lemma 6.2 twice, then Lemma 6.1 and use Jensen's inequality.

4. We define a function of  $\Delta\lambda$  giving the variance of  $X$  with respect to the measure  $\mu_q^*$ . We show that the right hand derivative of the function  $V(\Delta\lambda)$  is zero when  $\Delta\lambda = 0$  (**Lemma 6.5**).

$$V'_+(0) = \lim_{h \rightarrow 0^+} \frac{V(h+0) - V(0)}{h} = 0$$

We use this result to prove the next lemma.

5. The change in the expected value of the left peak of the invariant distribution is greater in magnitude than the change in the expected value of the right peak at  $\Delta\lambda = 0$  (**Lemma 6.6**).

$$\frac{dE_{\mu_p^*}[X]}{d\Delta\lambda} \geq -\frac{dE_{\mu_q^*}[X]}{d\Delta\lambda}$$

6. Which allows us to prove Theorem 4.2. By Lemma 6.6, for very small  $\Delta\lambda \geq 0$ ,  $E_{\mu_p^*}[X]$  increases faster than  $E_{\mu_q^*}[X]$  decreases in  $\Delta\lambda$ , implying that their mean,  $E[X]$ , increases with  $\Delta\lambda$ .

We provide some definitions of notation that will be used throughout the proof.

$$\text{for } \lambda \sim U[\bar{\lambda} - \Delta\lambda, \bar{\lambda} + \Delta\lambda], \quad g(\lambda) = \begin{cases} \frac{1}{\bar{\lambda} + \Delta\lambda - (\lambda - \Delta\lambda)} = \frac{1}{2\Delta\lambda}, & \bar{\lambda} - \Delta\lambda \leq \lambda \leq \bar{\lambda} + \Delta\lambda, \\ 0 & \text{otherwise} \end{cases}. \quad (6.1)$$

For values of  $\lambda$  greater than 3, the logistic map has two unstable fixed points at 0 and  $x_\lambda^* = 1 - \frac{1}{\lambda}$ , and two period-2 points,  $p_\lambda < q_\lambda$  at

$$p(\lambda) = \frac{\lambda + 1 - \sqrt{\lambda^2 - 2\lambda - 3}}{2\lambda}, \quad q(\lambda) = \frac{\lambda + 1 + \sqrt{\lambda^2 - 2\lambda - 3}}{2\lambda}. \quad (6.2)$$

Note that the fixed points are solutions of the quadratic:

$$\lambda x(1 - x) - x = 0$$

while the period-2 points are solutions to the quartic:

$$\lambda^2 x(1 - x)(1 - \lambda x(1 - x)) - x = 0$$

that are *not* fixed points.

$$p_\pm = p(\bar{\lambda} \pm \Delta\lambda) \quad q_\pm = q(\bar{\lambda} \pm \Delta\lambda) \quad (6.3)$$

The period-two points for  $\bar{\lambda} = 3.2$ ,  $\Delta\lambda = 0.1$ , are shown in Figure 8. Note that  $p_+ < p_-$  while  $q_- < q_+$ .

## 6.1 Proof of Theorem 4.2

The proof of Theorem 4.2 is divided up into several steps. First, we establish that, for small amplitudes of noise, the support of the invariant measure is contained in two disjoint intervals. This was discussed in Section 4.3.

Suppose the values of  $\lambda$  are in some interval  $[\bar{\lambda} - \Delta\lambda, \bar{\lambda} + \Delta\lambda]$ . Let  $I_p$  be the image under  $T(\vec{\lambda}, \cdot)$  of the interval of period-2 points,  $[q(\bar{\lambda} - \Delta\lambda), q(\bar{\lambda} + \Delta\lambda)]$ , and let  $I_q$  be the image of the other interval of period-2 points:  $[p(\bar{\lambda} + \Delta\lambda), p(\bar{\lambda} - \Delta\lambda)]$ . We will see that  $I_p \cap I_q = \emptyset$ .

**Lemma 6.1** *For  $\bar{\lambda} \in (3, 1 + \sqrt{6})$  with  $\Delta\lambda$  such that  $[\bar{\lambda} - \Delta\lambda, \bar{\lambda} + \Delta\lambda] \subset (3, 1 + \sqrt{6})$ , the support of the invariant distribution,  $I$ , is contained in the disjoint union  $I_p \cup I_q$ .*

**Proof** If  $\lambda \in (\bar{\lambda} - \Delta\lambda, \bar{\lambda} + \Delta\lambda)$ , with

$$3 < \bar{\lambda} - \Delta\lambda < \bar{\lambda} + \Delta\lambda < 1 + \sqrt{6} \quad (6.4)$$

then the dynamical system given by

$$x_{t+1} = S_\lambda(x_t) = \lambda x_t(1 - x_t)$$

has an asymptotically stable period-2 orbit [5] that attracts almost all orbits in  $[0, 1]$ . In other words, for a fixed value of  $\lambda$ , for almost all  $x_0 \in (0, 1)$  with respect to Lebesgue measure, the limit set of  $\{x_t\}_{t=0}^\infty$  is  $\{p(\lambda), q(\lambda)\}$  as given in Equation (6.2). This implies that almost all orbits of the stochastic map will approach a neighborhood of the set of period-2 points:  $[p_+, p_-] \cup [q_-, q_+]$ .

Let  $T(\vec{\lambda}, x)$  be the stochastic logistic map with  $\lambda \sim \mathcal{U}(\bar{\lambda} - \Delta\lambda, \bar{\lambda} + \Delta\lambda)$ , and let  $\mu^*$  be the unique stable invariant measure under  $T$ , as defined in Section 3.4. Denote the support of  $\mu^*$  by  $I$ . We will show that  $I \subset I_p \cup I_q$ , where are given by  $I_p = [x_{p,\min}, x_{p,\max}]$  and  $I_q = [x_{q,\min}, x_{q,\max}]$  as seen in Figure 9. We give an explicit description of  $I_p$  and  $I_q$  below.

For a fixed  $\bar{\lambda}$  and  $\Delta\lambda$  satisfying Equation (6.4), let  $p_\pm$  and  $q_\pm$  be defined as in Equation (6.3). Remember that, if a process is ergodic, the support of the unique invariant measure contains all invariant sets of positive measure. The stable period-2 points of  $S_\lambda(x)$  for all  $\lambda \in (\bar{\lambda} - \Delta\lambda, \bar{\lambda} + \Delta\lambda)$  must be contained in the support of  $\mu^*$  since these points are invariant under  $S_\lambda(x)$  for each  $\lambda \in (\bar{\lambda} - \Delta\lambda, \bar{\lambda} + \Delta\lambda)$ . Hence  $I \supset [p_+, p_-] \cup [q_-, q_+]$ . Figure 8 shows that  $I$  can, in fact, contain more than the set of stable period-2 points. This follows from the observation that the function  $S_\lambda(x)$  can be non-monotonic in the interval  $[p_+, p_-]$ , and the functions are decreasing on the interval  $[q_-, q_+]$  for  $\lambda \in (\bar{\lambda} - \Delta\lambda, \bar{\lambda} + \Delta\lambda)$ , so that  $S_{\bar{\lambda}_+}(q_-) > S_{\bar{\lambda}_-}(q_-) = p_-$ , and  $S_{\bar{\lambda}_-}(q_+) < S_{\bar{\lambda}_+}(q_+) = p_+$

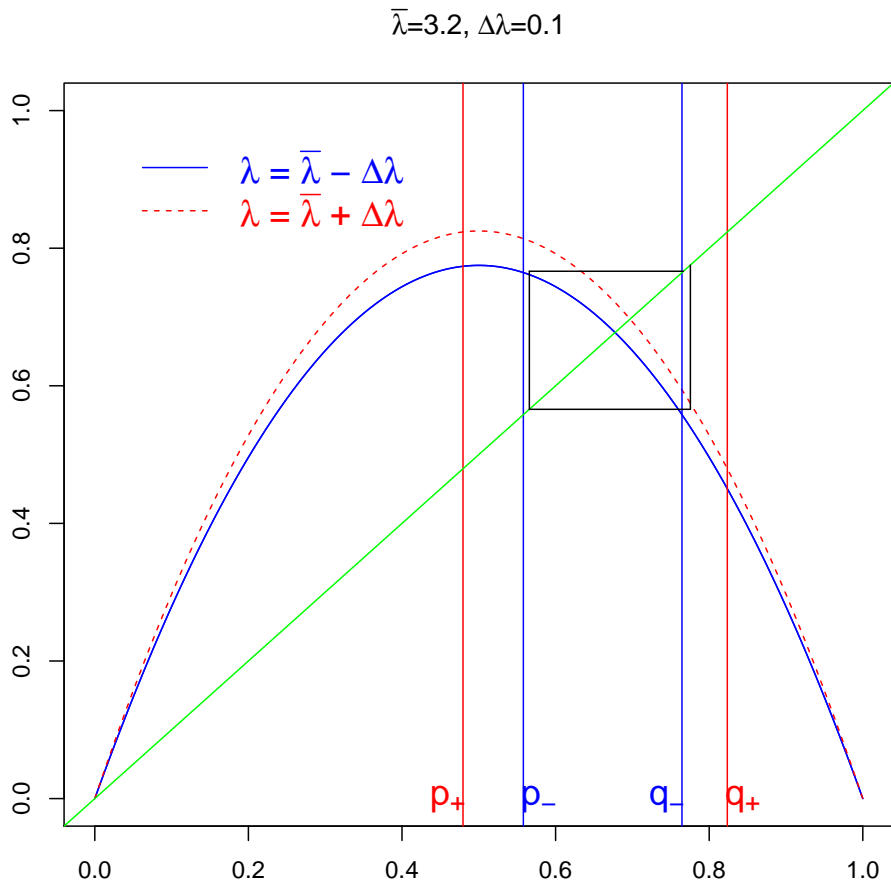


Figure 8: Two iterates of the stochastic logistic map,  $T(\vec{\lambda}, x)$  with initial value  $x_0 = .7755$  and parameter distribution  $\lambda \sim \mathcal{U}(3.1, 3.3)$ , i.e.,  $\bar{\lambda} = 3.2, \Delta\lambda = .1$ .

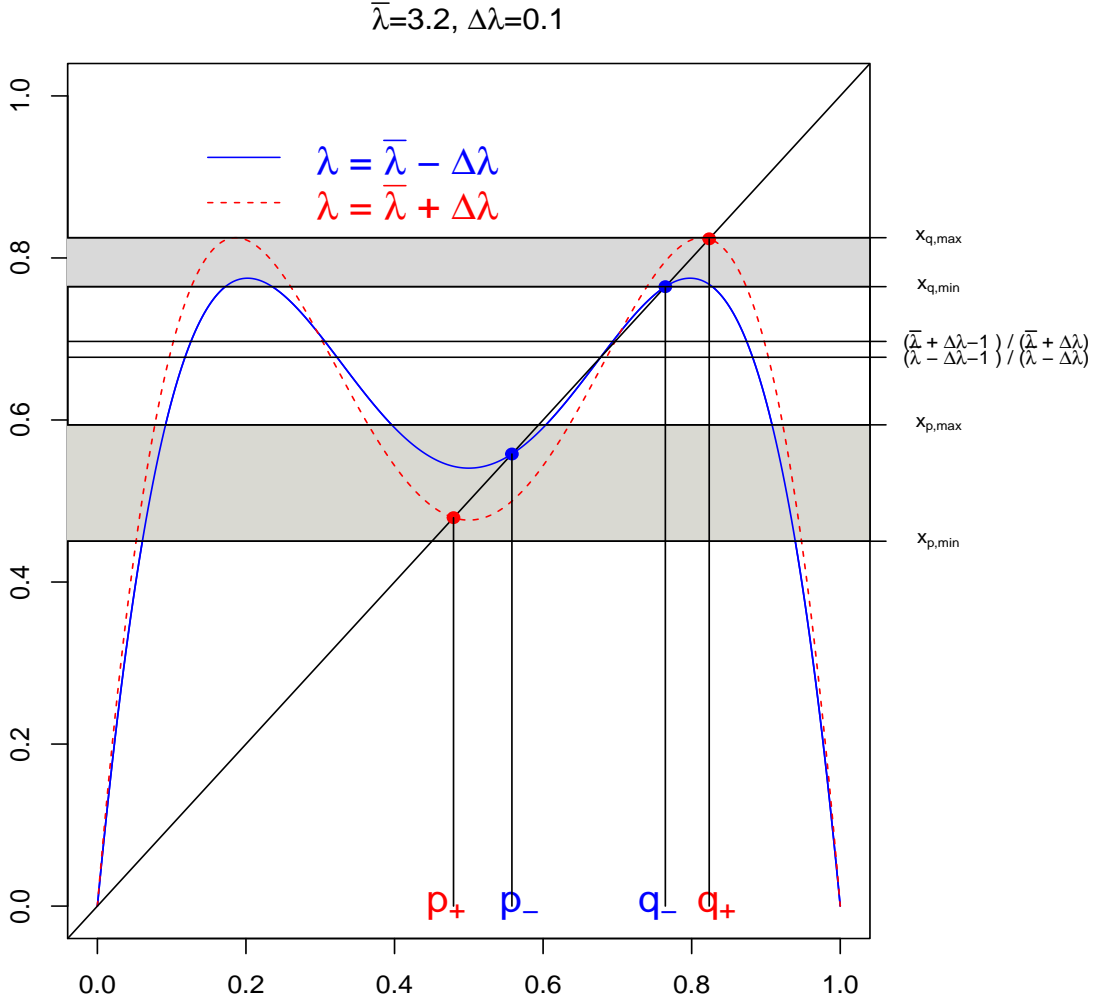


Figure 9: The disjoint intervals  $[x_{p,\min}, x_{p,\max}]$  and  $[x_{q,\min}, x_{q,\max}]$  are the images of  $[q_-, q_+]$  and  $[p_+, p_-]$ , respectively, under  $S_{\lambda_2}(S_{\lambda_1})(x)$  for all  $\lambda_{1,2} \in [\bar{\lambda} - \Delta\lambda, \bar{\lambda} + \Delta\lambda]$ .

For illustration, consider the case when  $1 + \sqrt{5} \in (\bar{\lambda} - \Delta\lambda, \bar{\lambda} + \Delta\lambda)$ , so that  $p_+ \leq \frac{1}{2} \leq p_-$  and the logistic map is non-monotonic on the interval  $[p_+, p_-]$ . Let  $x_t \in [p_+, p_-]$  and consider  $x_{t+1} = T(\bar{\lambda}, x_t)$ . We define  $x_{q,\min}$  to be the minimum value of  $x_{t+1}$ , so that  $x_{q,\min}$  is the smaller of  $q_-$  and  $S_{\bar{\lambda}-\Delta\lambda}(p_+)$ , noting that it is possible that  $x_{q,\min}$  can be smaller than  $q_-$ . Similarly, in this case the maximum value of  $x_{t+1}$  is  $x_{q,\max} = S_{\bar{\lambda}+\Delta\lambda}(\frac{1}{2}) = \frac{(\bar{\lambda}+\Delta\lambda)}{4}$ .

In general, define:

$$\begin{aligned}
 x_{p,\min} &= S_{\bar{\lambda}-\Delta\lambda}(q_+), & x_{p,\max} &= S_{\bar{\lambda}+\Delta\lambda}(q_-) \\
 x_{q,\min} &= \min\{q_-, S_{\bar{\lambda}-\Delta\lambda}(p_+)\}, & x_{q,\max} &= \max\{S_{\bar{\lambda}+\Delta\lambda}(1/2), S_{\bar{\lambda}+\Delta\lambda}(p_+), S_{\bar{\lambda}+\Delta\lambda}(p_-)\}
 \end{aligned} \tag{6.5}$$

These intervals are shown in Figure 9.

By writing  $x_{p,\max}$  and  $x_{q,\min}$  explicitly as functions of  $\lambda$  and  $\Delta\lambda$ , we see that the intervals  $I_p$  and  $I_q$  lie on either side of the non-zero fixed points corresponding to  $\bar{\lambda} + \Delta\lambda$  and  $\bar{\lambda} - \Delta\lambda$ , as follows:

$$p_+ < p_- = p(\bar{\lambda} - \Delta\lambda) \leq x_{p,\max} < \frac{\bar{\lambda} - \Delta\lambda - 1}{\bar{\lambda} - \Delta\lambda} < \frac{\bar{\lambda} + \Delta\lambda - 1}{\bar{\lambda} + \Delta\lambda} < x_{q,\min} \leq q_- = q(\bar{\lambda} - \Delta\lambda) < q_+ \quad (6.6)$$

so the intervals  $I_p$  and  $I_q$  are indeed disjoint. See Figure 9 which displays the ordered values given in Equation (6.6).  $\blacksquare$

Remark: the supports of  $\mu_p^*$  and  $\mu_q^*$  are contained in  $I_p$  and  $I_q$ , respectively. Lemma 6.1 therefore implies that all points in the support of  $\mu_p^*$  are mapped to the support of  $\mu_q^*$  under one iterate of  $T(\bar{\lambda}, x)$ , so that, by the definition of the Perron-Frobenius operator,  $P^* : \mu_p^* \mapsto \mu_q^*$  and vice-versa. Therefore, by construction,  $\mu^*(\text{support}(\mu_q^*)) = \mu^*(\text{support}(\mu_p^*)) = \frac{1}{2}$ .

**Lemma 6.2**

$$E_{\mu_q^*}[X] = E_{\mu_p^*}[S_{\bar{\lambda}}(X)].$$

when  $\lambda \sim U[\bar{\lambda} - \Delta\lambda, \bar{\lambda} + \Delta\lambda]$  with density  $g(\lambda)$  as given in Equation (6.1).

**Proof** We note that  $P^*\mu_p^*(x) = \mu_q^*(x)$ , where  $P^*$  is the Perron-Frobenius operator given in Equation (3.5). Therefore, we have:

$$E_{\mu_q^*}[X] = \int_0^1 x\mu_q^*(x) dx = \int_0^1 xP^*\mu_p^*(x) dx = \int_0^1 x \int_{V_x} \mu_p^*(y)g\left(\frac{x}{y(1-y)}\right) \frac{1}{y(1-y)} dy dx,$$

where the set  $V_x$  is  $\{(\lambda, y) : \lambda y(1-y) = x\}$ . Changing the order of integration, we have that:

$$E_{\mu_q^*}[X] = \int_0^1 \left[ \int_0^1 xg\left(\frac{x}{y(1-y)}\right) dx \right] \frac{1}{y(1-y)} \mu_p^*(y) dy.$$

The  $\lambda$ 's are uniformly distributed on  $[\bar{\lambda} - \Delta\lambda, \bar{\lambda} + \Delta\lambda]$  with  $g(\lambda)$  is as given in Equation (6.1). Using  $g(\lambda)$  in the expression for  $E_{\mu_q^*}[X]$  and evaluating the integral we get:

$$\begin{aligned} E_{\mu_q^*}[X] &= \int_0^1 \left[ \frac{x^2}{2} \Big|_{(\bar{\lambda}-\Delta\lambda)y(1-y)}^{(\bar{\lambda}+\Delta\lambda)y(1-y)} \frac{\mu_{p^*}(y)}{y(1-y)(2\Delta\lambda)} dy \right. \\ &= \int_0^1 \frac{((\bar{\lambda} + \Delta\lambda)^2 - (\bar{\lambda} - \Delta\lambda)^2) ((y(1-y))^2)}{2} \frac{\mu_{p^*}(y)}{y(1-y)(2\Delta\lambda)} dy \\ &= \bar{\lambda} \int_0^1 y(1-y)\mu_{p^*}(y) dy \end{aligned}$$

We can rewrite  $E_{\mu_q^*}[X]$  as:

$$E_{\mu_q^*}[X] = \bar{\lambda} \left( E_{\mu_{p^*}}[X] - E_{\mu_{p^*}}[X^2] \right) = \bar{\lambda} E_{\mu_{p^*}}[S_1(X)].$$

■

**Lemma 6.3** *The left peak of the invariant measure, i.e., the expected value with respect to  $\mu_p^*$ , is larger than the smaller point on the period-2 cycle of  $S_{\bar{\lambda}}$ .*

$$E_{\mu_p^*}[X] > p(\bar{\lambda}).$$

**Proof** Note that we are assuming that  $\Delta\lambda > 0$  in order to get a strict inequality. To prove Lemma 6.3, we introduce a new function,  $H_{\bar{\lambda}}(x)$ , which helps us put bounds on the second iterate of  $S_{\bar{\lambda}}(x)$ .

Fix values of  $\bar{\lambda}$  and  $\Delta\lambda$  in the period-2 regime:  $\bar{\lambda} \pm \Delta\lambda \in (3, 1 + \sqrt{6})$ .

Consider the functions  $F_{\bar{\lambda}}(x) = (S_{\bar{\lambda}} \circ S_{\bar{\lambda}})(x) - x$ , and  $H_{\bar{\lambda}}(x) = \bar{\lambda}h_{\bar{\lambda},\epsilon}(x) - x$  where

$$h_{\bar{\lambda},\epsilon}(x) = \bar{\lambda}x(1-x) - \bar{\lambda}^2(x(1-x))^2 + \epsilon \quad (6.7)$$

for some  $\epsilon > 0$ . From here on we drop the subscripts on  $h$  for clarity.

The function  $F_{\bar{\lambda}}(x)$  has four zeros. Two of the zeros are the two fixed points of  $S_{\bar{\lambda}}(x)$ : 0 and  $\frac{\bar{\lambda}-1}{\bar{\lambda}} = x^*(\bar{\lambda})$ ; two zeros are given by the period-2 orbit:  $p(\bar{\lambda})$  and  $q(\bar{\lambda})$ , as defined in Equation (6.2). We see that the function  $H$  is just a shift upward of the function  $F$  by  $\bar{\lambda}\epsilon$ :  $H(x) = F(x) + \bar{\lambda}\epsilon$ . If  $\epsilon$  is small enough,  $H$  will have the same number of zeros as  $F$ . If we label the zeros of  $H$  as:  $z_H < p_H < x_H^* < q_H$ , we have (see Figure 10):

$$z_H < 0 < p(\bar{\lambda}) < p_H < x_H^* < x^*(\bar{\lambda}) = \frac{\bar{\lambda}-1}{\bar{\lambda}} < q(\bar{\lambda}) < q_H < 1.$$

Now, fix  $\bar{\lambda}$ , and we will drop the subscript  $\bar{\lambda}$  on all the functions for readability.

Consider the region  $I_p$  which contains the support for  $\mu_p^*(x)$ , the left peak of the invariant measure. We note that  $h(I_p)$  is concave up, i.e.,  $h''(x) > 0$  for all  $x \in I_p$ . This implies by Jensen's Inequality that

$$E_{\mu_p^*}(h(X)) > h(E_{\mu_p^*}[X]) \Rightarrow E_{\mu_p^*}(h(X)) = h(E_{\mu_p^*}[X]) + \delta \quad \text{for some } \delta > 0. \quad (6.8)$$

Note that  $\delta$  is strictly greater than zero if  $h''(x)$  is strictly positive. The rest of the proof of Lemma 6.3 hinges on this fact.

**Claim 6.4** *The second derivative of  $h(x)$  is strictly positive for  $x \in I_p$ .*

**Proof** Let  $x_+^*$  and  $x_4^*$  be the non-zero fixed points of the function when  $\lambda = \bar{\lambda} + \Delta\lambda$  and  $\lambda = 4$ , respectively;  $q_4$  is the value of  $q(\lambda)$  given in Equation (6.2) evaluated at  $\lambda = 4$ . Note that  $I_p \subset [S_{\bar{\lambda}-\Delta\lambda}(q_+), x_+^*] \subset [S_3(q_4), x_4^*]$  since  $3 < \bar{\lambda} - \Delta\lambda < \bar{\lambda} + \Delta\lambda \leq 4$ . So it is sufficient to show that  $h''(x) > 0$  for all  $x \in [S_3(q_4), x_4^*] = [3q_4(1-q_4), \frac{3}{4}]$ . A direct calculation gives:

$$h''(x) = -2(\bar{\lambda} + \bar{\lambda}^2) + 12\bar{\lambda}^2(x - x^2) > -2(4 + 4^2) + 12 \cdot 3^2(x - x^2) = -40 + 108(x - x^2).$$

Multiplying by  $-\frac{1}{4}$ , we see that  $h''(x) > 0$  between the two roots of the quadratic  $27x^2 - 27x + 10$ . These

roots are:

$$r_{1,2} = \frac{27 \pm \sqrt{27^2 - 108}}{54}.$$

By direct calculation,

$$[r_1, r_2] \supset \left[ 3q_4(1 - q_4), \frac{3}{4} \right] \supset I_p.$$

Therefore,  $h''(x) > 0$  for all  $x \in I_p$ , which establishes Equation (6.8) with  $\delta > 0$ . ■

Now we return to the proof of Lemma 6.3. By applying Lemma 6.2 twice and using Equation (6.8) we get:

$$E_{\mu_q^*}[X] = E_{\mu_p^*}[S_{\bar{\lambda}}(X)] = E_{\mu_q^*}[S_{\bar{\lambda}}^2(X)] = \bar{\lambda}E_{\mu_q^*}[h(X)] - \bar{\lambda}\epsilon = \bar{\lambda}h(E_{\mu_q^*}[X]) + \bar{\lambda}(\delta - \epsilon).$$

Rearranging the equation, we have

$$\bar{\lambda}h(E_{\mu_q^*}[X]) - E_{\mu_q^*}[X] = \bar{\lambda}(\epsilon - \delta) = H(E_{\mu_q^*}[X]). \quad (6.9)$$

Since  $\epsilon$  can be arbitrarily small, we can make sure that  $0 < \epsilon < \delta$ , so that  $H(E_{\mu_q^*}[X]) < 0$ . This means that  $E_{\mu_q^*}[X]$  is either less than  $z_H < 0$ , greater than  $q_H$ , or in the interval  $(p_H, x_H^*)$  (see Figure 10). By Lemma 6.1, it is not possible for  $E_{\mu_p^*}[X]$  to be in the support of  $\mu_q^*$ , which implies that  $p_H < E_{\mu_q^*}[X] < x_H^*$ . Because  $H(x) > F(x)$ ,  $p(\bar{\lambda}) < p_H$ , from which we conclude that

$$E_{\mu_p^*}[X] > p(\bar{\lambda}) \quad (6.10)$$

and, as promised, the “left peak” shifts with noise added, i.e., when  $\Delta\lambda > 0$ . ■

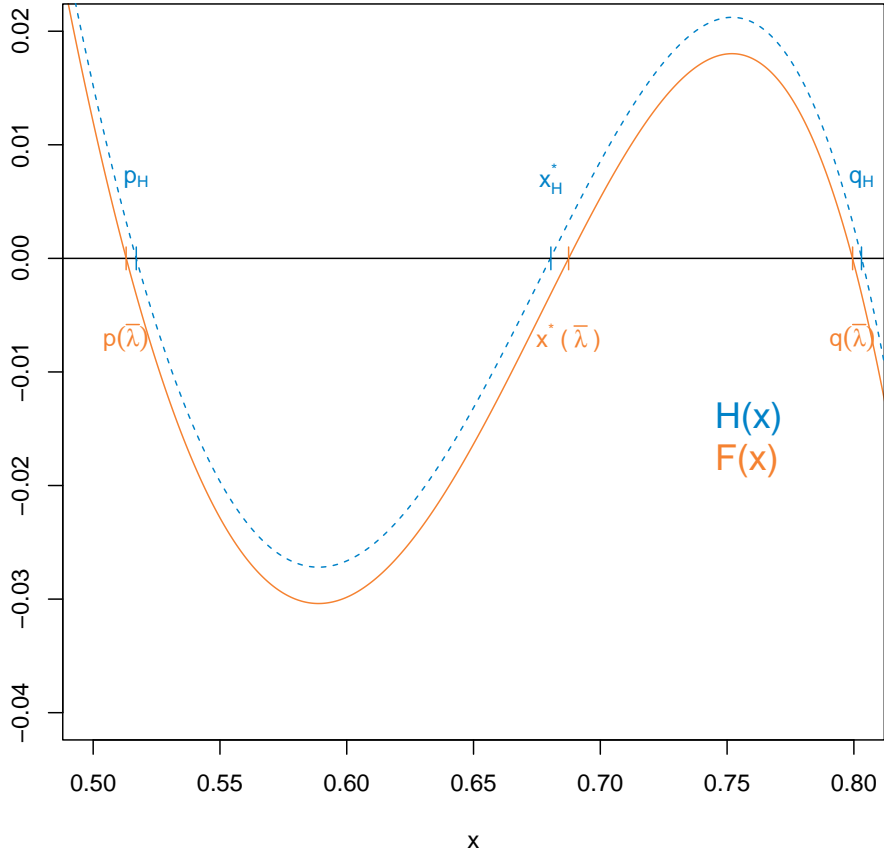


Figure 10:  $H(x)$  (dashed blue line) is the function which shifts  $F(x)$  (solid orange line) up by a small amount,  $\epsilon > 0$ . The curvature of the two functions is identical, but the zeros of  $H(x)$  are all shifted. In particular, the zero at  $p_H$  is to the right of  $p(\bar{\lambda})$ , which is the zero of  $F$  corresponding to the smaller period-2 point of  $S_{\bar{\lambda}}$ .

In this discussion, we fix  $\bar{\lambda}$  and consider values of the parameter,  $\lambda$ , uniformly distributed between  $\bar{\lambda} - \Delta\lambda$  and  $\bar{\lambda} + \Delta\lambda$ . We want to emphasize here and in what follows that the measures  $\mu_p^*$  and  $\mu_q^*$  are functions of  $\Delta\lambda$ , defined in Equation (4.1). In particular, we define a function:

$$V(\Delta\lambda) = E_{\mu_q^*(\Delta\lambda)}[X^2] - E_{\mu_p^*(\Delta\lambda)}[X^2]. \quad (6.11)$$

That is,  $V(\Delta\lambda)$  gives the variance of  $X$  with respect to the measure  $\mu_q^*$ , which is a function of  $\Delta\lambda$ . The variance function,  $V(\Delta\lambda)$  measures the difference between  $E_{\mu_q^*(\Delta\lambda)}[X^2]$  and  $E_{\mu_p^*(\Delta\lambda)}[X^2]$  as a function of  $\Delta\lambda$ .

The technical lemma, Lemma 6.5, is used to prove Lemma 6.6. We show directly that the right-hand derivative of the function  $V(\Delta\lambda)$  is zero when  $\Delta\lambda = 0$ . To show this, we use a very rough bound of the variance as the squared difference between the maximum and minimum values of the support of  $\mu_q^*$ .

**Lemma 6.5**

$$V'_+(0) = \lim_{h \rightarrow 0^+} \frac{V(h+0) - V(0)}{h} = 0$$

**Proof** We first note that  $V(0) = 0$ .

We consider the support of  $\mu_q^*(\cdot, \Delta\lambda, \bar{\lambda}) = (x_{q,\min}, x_{q,\max})$ , the right peak of the invariant distribution,  $\mu^*$ , in three distinct cases, and prove the lemma for each case separately.

Case 1 If  $\bar{\lambda} > 1 + \sqrt{5}$  and  $\Delta\lambda$  is sufficiently small, in which case  $x_{q,\min} = S_{\bar{\lambda}-\Delta\lambda}(p_+)$  and  $x_{q,\max} = S_{\bar{\lambda}+\Delta\lambda}(p_-)$ .

Case 2 If  $\bar{\lambda} < 1 + \sqrt{5}$  and  $\Delta\lambda$  is sufficiently small, in which case  $x_{q,\min} = q_-$  and  $x_{q,\max} = q_+$ .

Case 3 If  $\bar{\lambda} = 1 + \sqrt{5}$  in which case  $x_{q,\min} = q_-$  and  $x_{q,\max} = S_{\bar{\lambda}+\Delta\lambda}(\frac{1}{2})$ .

Case 1 We start with  $\bar{\lambda} > 1 + \sqrt{5}$ , which means that  $p(\bar{\lambda}) < \frac{1}{2}$ . For small enough  $\Delta\lambda$ , it follows that  $p_+ < p_- < \frac{1}{2}$ , i.e.,  $S_\lambda$  is monotonically increasing on the interval  $[p_+, p_-]$  for all  $\lambda \in [\bar{\lambda} - \Delta\lambda, \bar{\lambda} + \Delta\lambda]$ . This means that, for  $x_t \in [p_+, p_1]$ , the smallest possible value of  $x_{t+1}$  is  $S_{\bar{\lambda}-\Delta\lambda}(p_+) \triangleq x_{q,\min}$  and the largest possible value of  $x_{t+1}$  is  $S_{\bar{\lambda}+\Delta\lambda}(p_-) \triangleq x_{q,\max}$ .

It follows that the squared difference of the length of the interval from  $x_{q,\min}$  to  $x_{q,\max}$  gives a (rather crude) upper bound for the variance, i.e.,  $V(h) \leq (x_{q,\max} - x_{q,\min})^2$ . Thus:

$$\lim_{h \rightarrow 0^+} \frac{V(h)}{h} \leq \lim_{h \rightarrow 0^+} \frac{(S_{\bar{\lambda}-\Delta\lambda}(p_+) - S_{\bar{\lambda}+\Delta\lambda}(p_-))^2}{h}$$

Writing  $\Delta\lambda = h$ , and expressing everything in terms of  $q_+$  and  $q_-$ :

$$\begin{aligned} (S_{\bar{\lambda}-\Delta\lambda}(p_+) - S_{\bar{\lambda}+\Delta\lambda}(p_-))^2 &= ((\bar{\lambda} + h)p_-(1 - p_-) - (\bar{\lambda} - h)p_+(1 - p_+))^2 \\ &= ((\bar{\lambda} - h)p_-(1 - p_-) + 2hp_-(1 - p_-) - (\bar{\lambda} + h)p_+(1 - p_+) + 2hp_+(1 - p_+))^2 \\ &= \left( (q_+ - q_-) - 2h \left[ \frac{q_-}{\bar{\lambda} - h} + \frac{q_+}{\bar{\lambda} + h} \right] \right)^2 \\ &= (q_+ - q_-)^2 - 4h(q_+ - q_-) \left[ \frac{q_-}{\bar{\lambda} - h} + \frac{q_+}{\bar{\lambda} + h} \right] + \\ &\quad 4(h)^2 \left[ \frac{q_-}{\bar{\lambda} - h} + \frac{q_+}{\bar{\lambda} + h} \right]^2 \end{aligned} \tag{6.12}$$

We now divide both sides of Equation (6.12) by  $h$  and take the limit as  $h$  goes to zero:

$$\lim_{h \rightarrow 0^+} \frac{V(h)}{h} \leq \lim_{h \rightarrow 0^+} \left( \frac{(q_+ - q_-)^2}{h} - 4(q_+ - q_-) \left[ \frac{q_-}{\bar{\lambda} - h} + \frac{q_+}{\bar{\lambda} + h} \right] + 4(h) \left[ \frac{q_-}{\bar{\lambda} - h} + \frac{q_+}{\bar{\lambda} + h} \right]^2 \right) \tag{6.13}$$

Since  $\lim_{h \rightarrow 0^+} q_- = \lim_{h \rightarrow 0^+} q_+$ , we see that the middle term of Equation (6.13) goes to zero, and the last term goes to zero because  $h \rightarrow 0$ . Expanding the first term using Equation (6.2) gives:

$$q_+ - q_- = \frac{h}{(\bar{\lambda} + h)(\bar{\lambda} - h)} - \frac{(\bar{\lambda} + h)\sqrt{(\bar{\lambda} - h)^2 - 2(\bar{\lambda} - h) - 3}}{2(\bar{\lambda} + h)(\bar{\lambda} - h)} + \frac{(\bar{\lambda} - h)\sqrt{(\bar{\lambda} + h)^2 - 2(\bar{\lambda} + h) - 3}}{2(\bar{\lambda} + h)(\bar{\lambda} - h)}$$

Squaring and dividing by  $h$ :

$$\frac{(q_+ - q_-)^2}{h} = (A) + (B) + \frac{(C)}{(D)}$$

where

$$\begin{aligned} (A) &= \frac{h}{(\bar{\lambda} + h)^2(\bar{\lambda} - h)^2} \\ (B) &= \frac{1}{(\bar{\lambda} + h)(\bar{\lambda} - h)} \left[ \frac{(\bar{\lambda} - h)\sqrt{(\bar{\lambda} + h)^2 - 2(\bar{\lambda} + h) - 3}}{(\bar{\lambda} + h)(\bar{\lambda} - h)} - \frac{(\bar{\lambda} + h)\sqrt{(\bar{\lambda} - h)^2 - 2(\bar{\lambda} - h) - 3}}{(\bar{\lambda} + h)(\bar{\lambda} - h)} \right] \\ (C) &= (\bar{\lambda} - h)^2((\bar{\lambda} + h)^2 - 2(\bar{\lambda} + h) - 3) + (\bar{\lambda} + h)^2((\bar{\lambda} - h)^2 - 2(\bar{\lambda} - h) - 3) - \\ &\quad 2(\bar{\lambda} + h)(\bar{\lambda} - h)\sqrt{((\bar{\lambda} + h)^2 - 2(\bar{\lambda} + h) - 3)((\bar{\lambda} - h)^2 - 2(\bar{\lambda} - h) - 3)} \\ (D) &= 4h(\bar{\lambda} + h)^2(\bar{\lambda} - h)^2 \end{aligned}$$

Taking the limit as  $h$  goes to zero on both sides, we see that (A) is zero because of the  $h$  in the numerator; (B) is zero, since  $\bar{\lambda} - h \rightarrow \bar{\lambda} + h \rightarrow \bar{\lambda}$  as  $h \rightarrow 0^+$ . We can see that  $\frac{(C)}{(D)}$  also goes to zero as  $h \rightarrow 0^+$  by applying l'Hopital's rule. Therefore,  $\lim_{h \rightarrow 0^+} \frac{(q_+ - q_-)^2}{h} = \lim_{h \rightarrow 0^+} \frac{V(h)}{h} = 0$ .

Since the variance is always positive, we have:

$$0 \leq \lim_{h \rightarrow 0^+} \frac{V(h)}{h} \leq \lim_{h \rightarrow 0^+} \frac{(x_{q,max} - x_{q,min})^2}{h} = 0 \Rightarrow V'_+(0) = \lim_{h \rightarrow 0^+} \frac{V(h)}{h} = 0$$

when  $\bar{\lambda} > 1 + \sqrt{5}$ .

Case 2 Next, when  $\bar{\lambda} < 1 + \sqrt{5}$ , for small  $\Delta\lambda$ , the function  $S_\lambda(x)$  is increasing on the interval  $[p_+, p_-]$  for all  $\lambda \in [\bar{\lambda} - \Delta\lambda, \bar{\lambda} + \Delta\lambda]$ . It follows that  $x_{q,min} = q_-$  and  $x_{q,max} = q_+$  so the proof simplifies:

$$\lim_{h \rightarrow 0^+} \frac{V(h)}{h} \leq \lim_{h \rightarrow 0^+} \frac{(q_+ - q_-)^2}{h}.$$

It has already been shown that

$$\lim_{h \rightarrow 0^+} \frac{(q_+ - q_-)^2}{h} = 0,$$

therefore

$$0 \leq \lim_{h \rightarrow 0^+} \frac{V(h)}{h} \leq \lim_{h \rightarrow 0^+} \frac{(q_+ - q_-)^2}{h} = 0 \Rightarrow V'_+(0) = \lim_{h \rightarrow 0^+} \frac{V(h)}{h} = 0$$

when  $\bar{\lambda} < 1 + \sqrt{5}$ .

Case 3 Suppose  $\bar{\lambda} = 1 + \sqrt{5}$ , so that the maximum of the function coincides with the lower period-2 point when the parameter is  $\bar{\lambda}$ , i.e.,  $p(\bar{\lambda}) = \frac{1}{2}$ . We claim that in this case

$$\lim_{h \rightarrow 0^+} \frac{V(h)}{h} \leq \lim_{h \rightarrow 0^+} \frac{(S_{\bar{\lambda}+h}(1/2) - q_-)^2}{h}. \quad (6.14)$$

To see why this is true, we let  $f(x) = p(x) = \frac{x+1-\sqrt{x^2-2x-3}}{2x}$  be the smaller period-2 point when  $\lambda = x$ . We are interested in values of  $x$  near  $1 + \sqrt{5}$  that are in the stable period-2 regime, i.e.,  $3 < x < 1 + \sqrt{6}$ . We see that

$$f'(x) = \frac{-x-3-\sqrt{x^2-2x-3}}{2x^2\sqrt{x^2-2x-3}} < 0.$$

Furthermore,

$$f''(x) = \frac{x^3 + (\sqrt{x^2-2x-3}+3)x^2 - (2\sqrt{x^2-2x-3}+9)x - 3(\sqrt{x^2-2x-3}+3)}{x^3(x^2-2x-3)^{3/2}} > 0 \quad \text{when } x > 3.$$

We conclude that  $f(x)$  has negative slope and is concave up for  $x$  close to  $1 + \sqrt{5}$ , which means that  $f(1 + \sqrt{5} - \Delta\lambda)$  is farther from  $f(1 + \sqrt{5})$  than the distance from  $f(1 + \sqrt{5} + \Delta\lambda)$  to  $f(1 + \sqrt{5})$ . In other words,  $p_- - \frac{1}{2} > \frac{1}{2} - p_+$ . This implies that

$$x_{q,\min} = S_{\bar{\lambda}-\Delta\lambda}(p(\bar{\lambda} - \Delta\lambda)) = q_-.$$

We know that  $x_{q,\max}$  is the image of  $\frac{1}{2}$  under  $S_{\bar{\lambda}+\Delta\lambda}$ . Letting  $\Delta\lambda = h$  we have:

$$V(h) \leq (S_{\bar{\lambda}+h}(1/2) - q_-)^2$$

and Equation (6.14) is verified.

We now calculate the limit:

$$\lim_{h \rightarrow 0^+} \frac{V(h)}{h} \leq \lim_{h \rightarrow 0^+} \frac{(S_{\bar{\lambda}+h}(1/2) - q_-)^2}{h}.$$

Notice that the numerator in the second limit is zero, since, as  $h \rightarrow 0$ ,  $p_- \rightarrow \frac{1}{2}$

$$\Rightarrow q_- = S_{\bar{\lambda}-h}(p_-) \rightarrow S_{\bar{\lambda}}(1/2) = \lim_{h \rightarrow 0} S_{\bar{\lambda}+h}(1/2).$$

Therefore, we apply l'Hopital's rule to find:

$$\lim_{h \rightarrow 0^+} \frac{(S_{\bar{\lambda}+h}(1/2) - q_-)^2}{h} = \lim_{h \rightarrow 0^+} 2(S_{\bar{\lambda}+h}(1/2) - q_-) \frac{d}{dh} (S_{\bar{\lambda}+h}(1/2) - q_-)$$

This limit is zero as long as the last derivative term is finite. We verify this:

$$\begin{aligned} \frac{d}{dh} (S_{\bar{\lambda}+h}(1/2) - q_-) &= \frac{d}{dh} \left[ \frac{\bar{\lambda} + h}{4} - \frac{\bar{\lambda} - h + 1 - \sqrt{(\bar{\lambda} - h)^2 - 2(\bar{\lambda} - h) - 3}}{2(\bar{\lambda} - h)} \right] \\ &= \frac{1}{4} + \frac{1}{4(\bar{\lambda} - h)^2} \left[ 1 + \frac{h - \bar{\lambda} + 1}{2\sqrt{(\bar{\lambda} - h)^2 - 2(\bar{\lambda} - h) - 3}} 2(\bar{\lambda} - h) + 2 \left( \bar{\lambda} - h + 1 - \sqrt{(\bar{\lambda} - h)^2 - 2(\bar{\lambda} - h) - 3} \right) \right] \end{aligned}$$

We now take the limit as  $h \rightarrow 0$ , remembering that  $\bar{\lambda} = 1 + \sqrt{5}$ , so that  $\sqrt{\bar{\lambda}^2 - 3\bar{\lambda}} = 3 = 1$ , which gives:

$$\begin{aligned} \lim_{h \rightarrow 0} \frac{d}{dh} (S_{\bar{\lambda}+h}(1/2) - q_-) &= \frac{1}{4} + \frac{1}{4\bar{\lambda}^2} [1 + \bar{\lambda}(1 - \bar{\lambda}) + 2\bar{\lambda}] \\ &= \frac{1}{4} + \frac{1}{4\bar{\lambda}^2} [1 - \bar{\lambda}^2 + 3\bar{\lambda}] \\ &= \frac{1}{4} \left( \frac{1 + 3\bar{\lambda}}{\bar{\lambda}^2} \right) < \infty \end{aligned}$$

Therefore, by l'Hopital's rule, the limit is zero, and

$$\lim_{h \rightarrow 0^+} \frac{V(h)}{h} \leq \lim_{h \rightarrow 0^+} \frac{(S_{\bar{\lambda}+h}(1/2) - q_-)^2}{h} = 0$$

■

**Lemma 6.6** *The change in the expected value of the left peak of the invariant distribution is greater in magnitude than the change in the expected value of the right peak.*

$$\frac{dE_{\mu_p^*}[X]}{d\Delta\lambda} \geq -\frac{dE_{\mu_q^*}[X]}{d\Delta\lambda}$$

### Proof

From Lemma 6.5 we know that

$$\left. \frac{d}{d\Delta\lambda} \left[ E_{\mu_q^*}[X]^2 - E_{\mu_q^*}[X^2] \right] \right|_{\Delta\lambda=0} = V'_+(0) = 0$$

Because  $V'(\Delta\lambda)$  is continuous from above at zero <sup>1</sup> we know that there exists a  $\gamma$  such that  $|\gamma| < \frac{3-\bar{\lambda}}{\bar{\lambda}} \frac{d}{d\Delta\lambda} E_{\mu_q^*}[X]$  (note that  $3 - \bar{\lambda}$  and  $\frac{d}{d\Delta\lambda} E_{\mu_q^*}[X]$  are both negative, so their product is positive) and

<sup>1</sup>

$$\lim_{\Delta\lambda \rightarrow 0} V'(\Delta\lambda) = \lim_{\Delta\lambda \rightarrow 0} \lim_{h \rightarrow 0} \frac{V(\Delta\lambda + h)}{h} = \lim_{h \rightarrow 0} \frac{1}{h} \lim_{\Delta\lambda \rightarrow 0} V(\Delta\lambda + h) = 0$$

$$V'(\Delta\lambda) = \frac{d}{d\Delta\lambda} \left[ E_{\mu_q^*}[X]^2 - E_{\mu_q^*}[X^2] \right] = \gamma,$$

for  $\Delta\lambda$  small enough. Note that  $\gamma$  might be positive or negative, but for a small value of  $\Delta\lambda$  we can find a small enough  $\gamma$  in magnitude such that the two expected values are sufficiently close.

$$\begin{aligned}
\frac{d}{d\Delta\lambda} E_{\mu_p^*}[X] &= \bar{\lambda} \cdot \frac{d}{d\Delta\lambda} \left[ E_{\mu_q^*}[X] - E_{\mu_q^*}[X^2] \right], \text{ from Lemma 6.2} \\
&= \bar{\lambda} \cdot \frac{d}{d\Delta\lambda} \left[ E_{\mu_q^*}[X] - E_{\mu_q^*}[X^2] \right] + \bar{\lambda}\gamma \\
&= \bar{\lambda} \cdot \left[ \frac{d}{d\Delta\lambda} E_{\mu_q^*}[X] + 2E_{\mu_q^*}[X] \left( -\frac{d}{d\Delta\lambda} E_{\mu_q^*}[X] \right) \right] + \bar{\lambda}\gamma, \text{ note that } E_{\mu_q^*}[X] < 0 \\
&> \bar{\lambda} \cdot \left[ \frac{d}{d\Delta\lambda} E_{\mu_q^*}[X] + 2 \left( \frac{\bar{\lambda}-1}{\bar{\lambda}} \right) \left( -\frac{d}{d\Delta\lambda} E_{\mu_q^*}[X] \right) \right] + \bar{\lambda}\gamma, \text{ by defn of } \mu_q^*, E_{\mu_q^*}[X] > \frac{\bar{\lambda}-1}{\bar{\lambda}} \\
&= (2-\bar{\lambda}) \cdot \frac{d}{d\Delta\lambda} E_{\mu_q^*}[X] + \bar{\lambda}\gamma \\
&> (2-\bar{\lambda}) \cdot \frac{d}{d\Delta\lambda} E_{\mu_q^*}[X] + \bar{\lambda} \left( \frac{\bar{\lambda}-3}{\bar{\lambda}} \frac{d}{d\Delta\lambda} E_{\mu_q^*}[X] \right), \text{ because } \gamma > \frac{\bar{\lambda}-3}{\bar{\lambda}} \frac{d}{d\Delta\lambda} E_{\mu_q^*}[X] \\
&= -\frac{d}{d\Delta\lambda} E_{\mu_q^*}[X] \tag{6.15}
\end{aligned}$$

■

**Proof** of Theorem 4.2. From Lemma 6.3 we know that  $\frac{dE_{\mu_q^*}[X]}{d\Delta\lambda} < 0$ . Combining this with Lemma 6.6, it follows that  $\frac{dE_{\mu_p^*}[X]}{d\Delta\lambda}$  is both positive and greater in magnitude than  $\frac{dE_{\mu_q^*}[X]}{d\Delta\lambda}$ . Thus, for some interval around  $\Delta\lambda = 0$ ,  $E_{\mu_p^*}[X]$  is farther from  $p(\bar{\lambda})$  than  $E_{\mu_q^*}[X]$  is from  $q(\bar{\lambda})$ , implying that their mean,  $E[X]$ , is larger than the expected value of the deterministic map for  $\lambda = \bar{\lambda}$ . ■

## References

- [1] K.B. Athreya and Jack Dai. Random logistic maps. i. *Journal of Theoretical Probability*, 13(2):595–608, 2000.
- [2] K.B. Athreya and J.J. Dai. On the nonuniqueness of the invariant probability for i.i.d. random logistic maps. *The Annals of Probability*, 30(1):437–442, 2002.
- [3] N. Bacaër. *A Short History of Mathematical Population Dynamics*, chapter Verhulst and the logistic equation (1838). Springer, London, 2011.
- [4] Rabu Bhattacharya and Mukul Majumbar. *Random Dynamical Systems: Theory and Applications*. Cambridge University Press, Cambridge, 2007.
- [5] Robert Devaney. *Introduction to Chaotic Dynamics*. Addison-Wesley Pub., Reading, MA, 1989.

- [6] Persi Diaconis and David Freedman. Iterated random functions. *SIAM Review*, 41(1):45–76, 1999.
- [7] Kamil Erguler and Michael P.H. Stumpf. Statistical interpretation of the interplay between noise and chaos in the stochastic logistic map. *Mathematical Biosciences*, 216:90–99, 2008.
- [8] Haskell, C. and R. J. Sacker. The stochastic beverton-holt equation and the m. neubert conjecture. *Journal of Dynamics and Differential Equations*, 17(4):825–844, 2005.
- [9] Peter Hinow and Ami Radunskaya. Ergodicity and loss of capacity for a random family of concave maps. *Discrete and Continuous Dynamical Systems Series B*, 21(7):2193–2210, 2016.
- [10] Andrzej Lasota and Michael C. Mackey. *Chaos, fractals, and noise: stochastic aspects of dynamics*. Springer-Verlag, New York, 1994.
- [11] Robert M. May. Simple mathematical models with very complicated dynamics. *Nature*, 261:459–467, 1976.
- [12] Larry L. Rockwood. *Introduction to Population Ecology*. Blackwell Pub, Malden, MA, 2006.
- [13] Klaus Reiner Schenk-Hoppeé. Bifurcations of the randomly perturbed logistic map. Discussion Paper No. 252, Dept. of Economics, University of Bielefeld, 1997.
- [14] Steven H. Strogatz. *Nonlinear Dynamics and Chaos: With Applications to Physics, Biology, Chemistry, and Engineering*. Addison-Wesley Pub., Reading, MA, 1994.